SEISMIC RESPONSE ANALYSIS OF LEVEL SITES, EMBANKMENTS AND SOIL-STRUCTURE SYSTEMS

by

W.D. Liam Finn, M. Yogendrakumar, and A. Nichols

Department of Civil Engineering
University of British Columbia
Vancouver, B.C., Canada

ABSTRACT

Procedures for the analysis of site response and seismic soil-structure interaction are discussed in this paper. The reliability of these procedures is investigated by a number of case histories and data from simulated earthquake tests on centrifuged models. The results show that if the input motions can be characterized properly, seismic response can be predicted adequately for engineering purposes.

INTRODUCTION

The basic elements in the dynamic analysis of a soil-structure system are input motion, appropriate models of site and structure, constitutive relations for all materials present, and a stable, efficient, accurate, computational procedure. The specification of the input motion and the selection of an appropriate constitutive relation are the most difficult steps in the analysis.

Representative input motions are selected on the basis of magnitude and distance from source to minimize the amount of scaling required for application to the site under investigation. Candidate motions are usually scaled on the basis of peak acceleration although there is a trend to scaling

based on magnitude. It is recognized that high frequency motions attenuate faster than long period motions and that the period of peak spectral response shifts towards longer periods with distance from source. Therefore the candidate motions should have been recorded at distances which bracket the distance of the site from the epicentre of the design earthquake. Otherwise, the periods of peak response of the candidate motions should be scaled for distance. The chart developed by Seed et al. (1969) relating the predominant period of accelerations in rock with distance from the causative fault is useful for such scaling.

Linear elastic analysis is appropriate for low levels of shaking in relatively firm ground. As the shaking becomes more intense, soil response becomes nonlinear. A great variety of constitutive relations are available for nonlinear response analysis ranging from equivalent linear elastic models to elastic-plastic models with both isotropic and kinematic hardening. An additional complication is the effect of seismically induced porewater pressures. If these become significant, the corresponding reduction in effective stresses will result in significant reductions in moduli and strength which must be taken into account. Therefore, for some problems, the simpler total stress methods of analysis are not adequate; effective stress methods must be used.

The most widely used methods for dynamic analysis are based on the equivalent linear model. Computer programs representative of this approach are SHAKE (Schnabel et al., 1972) for one-dimensional analysis (1-D) and FLUSH (Lysmer et al., 1975) for 2-D analysis. These programs perform total stress analyses only. Equivalent linear models can exhibit pseudo-resonance, an amplification of computed response that is a function of the nature of the

model only. This phenomenon can lead to increased design requirements (Finn et al., 1978).

In recent years, there has been a distinct shift towards the use of nonlinear total or effective stress methods of analysis. A number of nonlinear 1-D programs are now available which give similar results for a given site (Streeter et al., 1973; Lee and Finn, 1975; Lee and Finn, 1978; Martin et al., 1978; Dikmen and Ghaboussi, 1984). A widely used program of this kind is DESRA-2 (Lee and Finn, 1978) and some field applications of this program will be discussed later.

A number of programs are also available for 2-D nonlinear dynamic effective stress analysis. The simplest kind are based on nonlinear hysteretic models of soil response using hyperbolic skeleton curves and unloading-reloading response defined by the Masing criterion (Masing, 1926). A representative program of this type is TARA-3, the third in an evolving series of TARA programs (Finn et al., 1986). This program has been subjected to critical evaluation over the last three years using data from centrifuge model tests sponsored by the U.S. Nuclear Regulatory Commission through the European Office of the U.S. Army Corps of Engineers. Some of these tests have been described previously by Finn (1986). Some results from this study will be presented later.

2-D elastic-plastic models for dynamic effective stress analysis are generally based on Biot's equations (Biot, 1941) for coupled fluid-soil systems. However few of these have been incorporated in commercially available programs. The most widely used program of this type is DYNAFLOW (Prevost, 1981). The elastic-plastic effective stress models offer the most complete description of soil response but the properties required in some of them are difficult to measure accurately and they make heavy demands on

computational time. Analyses using these models have been conducted on super computers to cut the turn around time.

ELASTIC RESPONSE ANALYSIS

Site response analyses are usually conducted to get site specific ground motion spectra for design, especially at soft sites. It is generally assumed that the most reliable results will be obtained if motions on local rock outcrops are available or can be estimated. These can be inputted at the rock-soil interface under the site.

An interesting example of this kind of analysis is provided by data from a Japanese site, (Ohta et al., 1977). The geological profile of the site is shown in Fig. 1a for a total depth of 3.5 km. The shear wave velocities are also given for the various soil and rock formations. The top 100 m of the formation is shown in Fig. 1b to a larger scale. A layer of soft material about 20 m thick with a low shear wave velocity exists at the surface. Below this layer the shear wave velocities generally exceed 400 m/s in the top 100 m of soil.

During an earthquake, accelerations were measured in the base rock at a depth of 3.5 km and at various elevations up to the surface. Analysis of the site was conducted using the base rock motions as input. The soils were assumed to respond elastically because of the low level of excitation. The computed accelerations at various elevations are compared with the recorded accelerations in Fig. 2. The computed motions agree very well with the recorded motions except in the soft layer near the surface where the computed motions greatly underestimate the recorded motions. Decomposition of the measured ground motions at the surface showed that surface waves of the Love

type existed in the soft surface layer. These waves were separated from the recorded motions as shown in Fig. 3. When these motions are added to the computed surface accelerations, the computed and measured surface motions agree very closely. This example is especially interesting because motions were recorded from bedrock to surface. Therefore there was none of the usual uncertainty about base input motion. Yet the predictions of surface motions were poor. In this case the contribution to surface motions from shear waves propagating vertically were accurately predicted but there was an additional component of motion which was not represented in the modelling process, the surface wave.

This example suggests that the common practice of using rock outcrop motions as input motions to soft sites should be followed with caution. Additional evidence of difficulties with this procedure are given in the next section.

EQUIVALENT LINEAR ANALYSIS OF MEXICO CITY SITES

Mexico City is located in the South West corner of the Valley of Mexico on the edge of the former Lake Texcoco. During the 1985 earthquake, ground accelerations were recorded on hard sites in the foothills of the University district (UNAM) and on the soft deposits of the old lake bed. The locations of the accelerograph sites discussed in this paper are shown in Fig. 4. The recorded data provide an opportunity to check the reliability of the usual procedures for conducting site response analysis.

Soil conditions in the lake zone are characterized by soft clay deposits overlying dense sands and much stiffer clays with shear wave velocities comparable to those of soft rock. Romo and Seed (1986) characterized the

lake zone sites as homogeneous clay layers with the properties shown in Table 1. The CAF and CAO sites are located in Central de Abastos (Fig. 4). The shear wave velocities, V_s, were

Site	Depth	Shear Wave Velocity	Unit Weight
SCT	35-40 m	75-80 m/s	1.2 t/m^3
CAO	55 m	65-75 m/s	1.2 t/m^3
CAF	45 m	70 m/s	1.2 t/m^3

Table 1. Properties of Mexico City Sites for Dynamic Analysis (after Romo and Seed, 1986).

determined from the Fourier spectra of the recorded motions (Romo and Seed, 1986). The corresponding shear moduli, G, were obtained from $G = \rho V_s^2$ in which ρ = mass density of the soil. These values compared well with moduli derived from the results of resonant column and cyclic triaxial tests (Romo and Jaime, 1986). The variations of shear modulus and damping of Mexico City clay as a function of shear strain (Leon et al., 1974; Romo and Jaime, 1986) are shown in Fig. 5.

The response of the lake zone sites will be analyzed in two ways, (1) following the usual procedure of using an appropriately scaled acceleration record from another earthquake as a representative input motion and (2) using the rock outcrop motions recorded at UNAM.

Analysis Using Scaled Motion

Romo and Seed (1986) analysed the three lake bed sites using the program SHAKE (Schnabel et al., 1972). They used the Pasadena record of the 1952 Kern County earthquake (M = 7.6) as a representative input motion after scaling it appropriately for peak acceleration and frequency to obtain strong

response around a period of two seconds, the period of the SCT site. This scaling resulted in a good match between the computed acceleration response spectrum for the SCT site and the average spectrum of the two horizontal components of acceleration recorded at the site (Fig. 6). This analysis was repeated for the present study and similar results were obtained (Fig. 6).

The acceleration response spectrum of the scaled Pasadena motions is shown in Fig. 7 together with the spectrum of the motions scaled for peak acceleration only. It is clear that scaling for frequency resulted in a major shift in the period of strong spectral response. Such a major scaling for frequency would probably not have been considered necessary had it not been for the availability of the 1985 ground motion records which showed that the peak response at the SCT site occurred around a period of 2 sec and that the rock motion had relatively high response at the same period. The predominant period of rock input motions would probably have been estimated at around 1.5 sec based on the relationship between predominant period and distance to the causative fault developed by Seed et al. (1969). Note that uniform scaling of a record for frequency does more than simply shift the period of peak response to the desired frequency. It also enlarges the frequency range in which strong response may be encountered. Therefore input motions with predominant periods greatly different from the required predominant period should not be uniformly scaled unless broad band strong response is desired.

Analysis Using Rock Outcrop Motions

Accelerations were recorded at two hard sites at UNAM. The motions, designated CUOl and CUIP, were recorded on the first floor of a three storey building and in the free field respectively. The seismic response of the SCT

site was analyzed using the N90W and N00E components of these motions as input motions to the SHAKE program.

The acceleration response spectra for the computed ground motions are compared with the corresponding spectra of the recorded motions in Figs. 8 and 9. In the N90W direction, both spectra of the computed motions underestimate the spectrum of the recorded motions both in terms of peak spectral acceleration and the range of strong response (Fig. 8). The agreement in the case of the N00E components is much better (Fig. 9). Clearly the motions at the SCT site must have a much greater directional bias than the rock motions recorded at UNAM. This is evident from the acceleration plots in Figs. 10a and 10b, which show the total acceleration paths for the CUIP motions at the UNAM site and the SCT site respectively. Note that the acceleration paths for the SCT site lie in an elongated band inclined significantly more to the E-W direction than to the N-S direction.

A close match between the computed and measured spectra for the N90W direction is obtained if the CUIP input motions are scaled to a peak acceleration of 0.095 g from 0.035 g as shown in Fig. 11. Note that the peak spectral accelerations are approximately equal and the range of peak response is now considerably wider than that obtained using the unscaled motions as input (Fig. 8). Even the shoulder in the recorded response spectrum to the right of the peak response is now reproduced. When the N90W component of the CU01 motions are scaled also to 0.095 g, the computed response is slightly greater than the recorded response but the correct shape is reproduced. By further refinement in the scaling a closer match could be obtained in the region of peak response. But the lesson is already clear that scaling of the rock outcrop motions by a factor of about 2.5 is necessary to get a good match between recorded and computed spectra in the N90W direction in the

region of peak response. Note that the scaling to match peak response has resulted in higher computed responses around a period of 1 sec. It is not possible to get simultaneously a good match in both these regions of the response spectrum. A reasonable match may be obtained in the N-E direction with little or no scaling (Fig. 9).

The strong response at the SCT site around a period of 2 sec (Fig. 8) is due to the coincidence of the predominant period of strong input shaking with the fundamental period of the site. The free field motions recorded at UNAM showed a relatively strong response around a period of 2 sec (Fig. 12). However this is not simply the effect of distance from the source. The acceleration spectrum of the motions recorded at Caleto de Campos only 21 km from the epicentre shows a very strong response already present around a period of 2 sec (Fig. 13). These results suggest that source mechanism as well as magnitude and distance from the site may play a significant role in determining the frequencies of rock outcrop motions. Therefore the source mechanism should be matched also when selecting representative input motions.

The seismic response of the CAF site was analyzed using the N90W and N00E components of the unscaled CUIP rock motions as input. The computed acceleration response spectra are compared with the spectra of the corresponding recorded motions in Figs. 14 and 15. The spectral shapes are significantly different and no scaling of the input motions for peak acceleration will result in good agreement between spectra for computed and recorded motions of the N00E component. However, the average spectrum of the recorded motions can be matched remarkably well using the same scaled Pasadena record used in the analysis of the SCT site as shown in Fig. 16. Similarly at the CAO site, the average spectrum of the recorded motions can

be matched reasonably well using the Pasadena record but the spectra of the recorded motions at the site cannot be matched if the rock outcrop motions are used as input.

There are a number of possible explanations for the discrepancies between recorded and computed spectra when the rock outcrop motions are used as input. If it is assumed that the shear beam model adequately represents the dynamic response of the sites then it must be assumed that the rock outcrop motions are modified as they pass into the hard sand layer, acquiring a directional bias and a redistribution of peaks. But it seems unlikely that this is the sole explanation. It is probable that surface waves are generated in the stratum above the sand layer with periods dependent on the local thickness and stiffness of the layer. Information on these waves would not be included in the rock outcrop motions, resulting in significant long period differences between computed and recorded responses.

1-D NONLINEAR DYNAMIC EFFECTIVE STRESS ANALYSES

The distinguishing characteristic of effective stress methods is the capability of predicting seismically induced porewater pressures and taking their effects into account during analysis. The DESRA-2 program has been used to evaluate site response at a number of sites in Japan (Finn et al., 1982; Iai et al., 1985) at which seismic porewater pressures were measured or liquefaction occurred. Some results from these studies are presented in the next section.

Seismic response of Owi Island test site

Owi Island test site

Owi Island No. 1 is an artificial island located on the west side of Tokyo Bay. A test site at the south end of the island is instrumented to record porewater pressures and ground accelerations during earthquakes. Porewater pressures are recorded by piezometers installed at depths of 6 m and 14 m. The transducer in each recorder is of the strain-gauge type with a full capacity of 200 kN/m^2. A two-component seismograph is installed on the ground surface to measure horizontal acceleration. The soil profile at the site, is shown in Fig. 17. The sand layers in which the piezometers were embedded at depths of 6 m and 14 m had almost identical blow counts of N = 5. The depths from which undisturbed samples were recovered are also shown in Fig. 17.

The Mid-Chiba earthquake, with a magnitude M = 6.1, shook the Tokyo Bay area on September 25, 1980. The ground shaking, due to the earthquake, was of intensity V on the Japanese Meterological Agency Scale in the Tokyo Bay area and was sufficient to develop the porewater pressures and accelerations shown in Fig. 18. The maximum horizontal accelerations at the ground surface were 95 gals in the N-S direction and 65 gals in the E-W direction. The rise in porewater pressure was 0.75 m of water in the sand layer at a depth of 6 m and 1.32 m at a depth of 14 m. Fourier spectra of the acceleration records indicate that the predominant periods of motion were 0.64 sec and 0.5 sec in the E-W and N-S directions, respectively.

All the properties required for the analysis of Owi Island No. 1 by DESRA-2 were obtained using data usually available from conventional site and laboratory investigations.

Full details of the instrumentation, recorded data, and the site investigations on Owi Island and the associated laboratory testing have been described by Ishihara et al. (1981). A more detailed description of the analysis of the site is by Finn et al. (1982).

Comparison of Field and Computed Responses

The recorded ground motions are shown in Fig. 19a; those computed by DESRA-2 in Fig. 19b. Except for minor differences in frequency and magnitude in the 8-10 s range, the computed record is very similar to the recorded motions.

The porewater pressures recorded at the 6 m depth are shown to an expanded scale in Fig. 20a. During the low level shaking of the first 4 s, the response was elastic and porewater pressures developed in instantaneous response to changes in the total applied mean normal stresses. Such porewater pressures result from the elastic coupling of soil and water. With the onset of more severe shaking, plastic volumetric strains are induced and these result in the development of residual porewater pressures which are independent of the instantaneous states of stress. These pressures accumulate with continued plastic volumetric deformation. Residual porewater pressure is indicated by the steep rise and sustained level in recorded porewater pressure in Fig. 20a. During shaking, the varying applied stresses continue to generate small instantaneous fluctuations in the porewater pressure which are superimposed on the larger residual porewater pressures. The gradual decay in the sustained level of porewater pressure is due to dissipation of porewater pressure by drainage. At this stage in the excitation, the dissipation of porewater pressure by drainage exceeds the generation by low level excitation.

The computed porewater pressures are shown in Fig. 20b and are very similar to the recorded values. DESRA-2 computes only residual porewater pressures so there are no fluctuations in the computed pressures due to changes in instantaneous stress levels.

Recorded and computed porewater pressures for the sand layer at a depth of 14 m are shown in Figs. 21a and 21b, respectively. DESRA-2 results compare very favourably with the recorded values. Dissipation of porewater pressure is negligible in the lower sand compared to the upper sand because it is capped by a clay layer instead of by pervious fill. The DESRA-2 program can take these different drainage conditions into account during the dynamic analysis.

The Port and Harbour Research Institute of Japan investigated the liquefaction potential of 6 sites at the port of Ishinomaki using the program DESRA-2 (Iai et al., 1985). Four of the sites, A,B,D and F liquefied during the 1978 Miyagi-Ken-Oki earthquake. Sites C and E did not liquefy. Results from the DESRA-2 analyses agreed with the field experience as may be seen in Fig. 22. Liquefaction is indicated by $u/\sigma'_{vo} = 1$.

2-D NONLINEAR DYNAMIC EFFECTIVE STRESS ANALYSIS

2-D dynamic analyses are usually conducted using equivalent linear finite element analyses in the frequency domain. There has been little verification of these methods because of a lack of adequate field data.

There are certain important phenomena in soil-structure interaction outside the scope of conventional frequency domain analysis. Typical examples are uplift during rocking, permanent deformations, the effects of

seismically induced porewater pressures, hysteretic behaviour and stick-slip behaviour at interfaces between structure and foundation soils.

The program TARA-3 (Finn et al., 1986) was developed to cope with such problems. The capability of the program will be demonstrated by using it to analyze one of the NRC centrifuge tests which models the response of a heavy two-dimensional structure embedded in a saturated sand foundation to seismic excitation.

ANALYSIS BY TARA-3

In TARA-3, response in shear is assumed to be nonlinear and hysteretic with unloading and reloading stress-strain paths defined by the Masing criterion (Masing, 1926). The response of the soil to uniform all round pressure is assumed to be nonlinearly elastic and dependent on the mean normal effective stress. Porewater pressures during shaking are computed using the Martin-Finn-Seed porewater pressure model (Martin et al., 1975) modified to take into account the effects of initial static shear stress. Moduli and strength are continuously modified during analysis to reflect changes in the effective stress regime. A detailed description of the constitutive relations in TARA-3 is given by Finn (1985).

For analysis involving soil-structure interaction it may be important to model slippage between the structure and soil. Slip may occur during very strong shaking or even under moderate shaking if high porewater pressures are developed under the structure. TARA-3 contains slip elements of the Goodman (Goodman et al., 1968) type to allow for relative movement between soil and structure in both sliding and rocking modes during earthquake excitation.

TARA-3 ANALYSIS OF EMBANKMENTS

A static analysis is first carried out to determine the stress and strain fields througout the dam cross-section. The deformed shape of a submerged embankment of sand at a relative density D_r = 50% as computed by TARA-3 is shown in Fig. 23. Dynamic analysis in each element of the dam starts from the static stress-strain condition. This leads to accumulating permanent deformations in the direction of the smallest residual resistance to deformation. Methods of dynamic analysis commonly used in practice ignore the static strains in the dam and start from the origin of the stress-strain curve in all elements even in those which carry high shear stresses.

As shaking proceeds, two phenomena occur; porewater pressures develop in saturated portions of the embankment and, in the unsaturated regions, volumetric strains and associated settlements develop. The program takes into account the effects of the porewater pressures on moduli and strength during dynamic analysis and estimates the additional deformations due to gravity acting on the softening soil. At the end of the earthquake, additional settlements occur due to consolidation as the seismically induced residual porewater pressures dissipate. The final deformed shape of the dam results from the sum of permanent deformations due to the hysteretic dynamic stress-strain response, constant volume deformations in saturated portions of the embankment, volumetric strains in unsaturated portions and deformations due to consolidation as the seismic porewater pressures dissipate. The final post-earthquake deformed shape of the saturated embankment computed by TARA-3 is shown in Fig. 24. This shows the classical spreading due to high porewater pressures.

The post-earthquake deformed shape of an embankment with a central core is shown in Fig. 25. The water table is about 5 ft below the crest. Only the upstream segment to the left of the core is saturated and generates high porewater during earthquake shaking. Large deformations occur upstream and the core is strongly deformed towards the upstream side. Although the deformations in this case are contained, they are sufficient to cause severe cracking around the core.

These examples show the ability of TARA-3 to predict at least phenomenologically observed deformation modes in embankments. It remains to be shown that it can also make useful quantitative predictions of all important characteristics of seismic response.

VALIDATION OF TARA-3

The United States Nuclear Regulatory Commission (USNRC) through the European Research Office of the U.S. Army sponsored a series of centrifuged model tests to provide data for the validation of the TARA-3 program. The tests were conducted on the large geotechnical centrifuge at Cambridge University in the United Kingdom. Details of the Cambridge centrifuge and associated procedures for seismic tests have been described by Schofield (1981). Data from some of these tests wil be described and analyzed to validate the capability of TARA-3. Further details may be found in Finn (1985) and Finn et al. (1984,1985a,1985b). The tests described below are chosen to illustrate the capability of TARA-3 to predict, porewater pressures, settlements and accelerations.

SEISMIC RESPONSE OF A SATURATED EMBANKMENT

A plane strain model of a saturated submerged embankment is shown in Fig. 26. The model is 110 mm high with side slopes 2.2 to 1 and a crest width of 236 mm. The centrifuge acceleration used in the test was nominally 80 g. The model, therefore, corresponds to a prototype 8.8 m high with a crest width of 18.8 m. The model was instrumented by 8 DJB A23 piezoelectric accelerometers (ACC), 10 Druck PDCK 81 pore pressure transducers (PPT). The locations of the instruments for which results will be presented are shown in Fig. 26.

The embankment was constructed with Leighton-Buzzard sand passing British Standard Sieve (BSS) No. 120 and retained on BSS No. 200. The relative density of the embankment sand was D_r = 65%. The liquefaction potential of the sand was determined by cyclic simple shear tests using the University of British Columbia simple shear device. The liquefaction curve for a relative density D_r = 65% is shown in Fig. 27.

De-aired silicon oil with a viscosity of 80 centistokes was used as a pore fluid in order to model the drainage conditions in the prototype during the earthquake. If the linear scale factor between model and prototype is N, then excess porewater pressures dissipate approximately N^2 times faster in the model than in the prototype if the same fluid is used in both. The rate of loading by seismic excitation will be only N times faster. Therefore, to model prototype drainage conditions during the earthquake, a pore fluid with a viscosity N times the prototype viscosity must be used. This viscosity was achieved by an appropriate blending of commercial silicon oils. Tests by Eyton (1982) have shown that the stress-strain behaviour of fine sand is not changed when silicon oil is substituted for water as a pore fluid.

Typical Test Data

Signals from the model were recorded on a 14-track RACAL tape recorder. These analog signals were processed and digitized using the software package, FLY-14, developed by Dean (1985). The raw digitized data was smoothed once using a three-point average scheme taking 1/2 of the value at the current point, 1/4 of the value at the previous point, and 1/4 of the value at the next point. This was necessary to filter out very high frequency electrical noise which contained negligible energy.

Samples of test data for a peak input acceleration of 0.16 g are shown in Fig. 28. It should be noted that there are wide variations in the scales of the various transducer records so that each record may be accommodated in the same sized data box. The apparently quite different forms of some of the records are due primarily to these differences in scales. All scales are model scales. The accelerations are expressed as percentages of the centrifuge acceleration. Porewater pressures are those actrually measured.

Analysis by TARA-3

The dynamic response of the model embankment was analyzed using TARA-3. Computed and measured accelerations are shown in Fig. 29 for ACC 1258 near the crest of the embankment and in Fig. 30 for ACC 2033 located in the lower half of the embankment. The computed and measured acceleration records are very similar in frequency content and the peak accelerations are satisfactorily predicted by TARA-3.

The computed porewater pressures for PPT 2331 located near accelerometer ACC 2033 are compared with the measured porewater pressures in Fig. 31. TARA-3 models the residual porewater pressure quite well as may be seen by comparing the peak computed porewater pressure with the measured pressure at

the end of the earthquake. The elastic fluctuations in porewater pressure due to transient changes in the total mean normal stresses are not modelled. The stability and stiffness of the soil depend on the residual porewater pressures mostly and therefore the complexities involved in modelling the coupled analysis that would be required to predict the transient fluctuations are now warranted.

Very good agreement is also found between the computed and measured porewater pressures for the gauge PPT 2342 located in the vicinity of ACC 1258 (Fig. 32). It appears that TARA-3 can model the effective stress response of saturated embankments adequately.

SEISMIC RESPONSE OF A DRY EMBANKMENT

A model of an embankment of dry sand is shown in Fig. 33. The embankment is 105 mm high with a crest width of 230 mm. The model is 480 mm thick. It was constructed of Leighton Buzzard Sand, passing British Standard Sieve (BSS) No. 120 and retained on BSS No. 200, to a uniform relative density D_r = 70%.

The embankment carries a steel plate 15 mm thick and 65 mm wide which exerts a pressure of 92 kPa on the embankment. The plate acts as a firm platform for the measurement of settlement.

Horizontal accelerations were recorded by DJB A23 piezo-electric accelerometers (ACC), the locations of which are shown in Fig. 33. Also shown in Fig. 33 are the locations of LVDT's for measuring settlement. The LVDT's on the slopes did not perform satisfactorily because of the initial irregular surfaces of the slopes and the effects of wind erosion during

centrifuge flight. Therefore no data are reported from these LVDT's in any of the centrifuge tests.

The seismic tests on the model were conducted at a nominal centrifugal acceleration of 80 g. The model, therefore, simulated an embankment 8 m high with a crest width of 18 m.

For this test interest is focussed on the capability of TARA-3 to predict settlements of the embankment, so only settlement data will be shown. The computed and measured settlements tabulated in Fig. 34 show very good agreement. The post-earthquake deformed shape of the embankment is also shown in Fig. 34.

RESPONSE OF SATURATED EMBANKMENT WITH EMBEDDED STRUCTURE

A schematic view of a saturated embankment with an embedded structure is shown in Fig. 35. This configuration with strong soil-structure interaction provides a very severe test of the capabilities of TARA-3 to model dynamic response. The structure is made from a solid piece of aluminum alloy and has dimensions 150mm wide by 108mm high in the plane of shaking. The length perpendicular to the plane of shaking is 470mm and spans the width of the model container. The structure is embedded a depth of 25mm in the sand foundation. Sand was glued to the base of the structure to prevent slip between structure and sand.

The foundation was constructed of Leighton Buzzard Sand passing BSS No. 52 and retained on BSS No. 100. The mean grain size is therefore 0.225mm. The sand was placed as uniformly as possible to a nominal relative density D_r = 52%.

During the test the model experienced a nominal centrifugal acceleration of 80 g. The model therefore simulated a structure approximately 8.6m high by 12m wide embedded 2m in the foundation sand.

De-aired silicon oil with a viscosity of 80 centistokes was used as a pore fluid. In the gravitational field of 80g, the structure underwent consolidation settlement which led to a significant increase in density under the structure compared to that in the free field. This change in density was taken into account in the analysis.

The locations of the accelerometers (ACC) and pressure transducers (PPT) are shown in Fig. 36. Analyses of previous centrifuge tests indicated that TARA-3 was capable of modelling acceleration response satisfactorily. Therefore, in the present test, more instrumentation was devoted to obtaining a good data base for checking the ability of TARA-3 to predict residual porewater pressures.

As may be seen in Fig. 36, the porewater pressure transducers are duplicated at corresponding locations on both sides of the centre line of the model except for PPT 2255 and PPT 1111. The purpose of this duplication was to remove any uncertainty as to whether a difference between computed and measured porewater pressures might be due simply to local inhomogeneity in density.

The porewater pressure data from all transducers are shown in Fig. 37. These records show the sum of the transient and residual porewater pressures. The peak residual pressure may be observed when the excitation has ceased at about 95 milliseconds. The pressures recorded at corresponding points on opposite sides of the centre line such as PPT 2631 and PPT 2338 are generally quite similar although there are obviously minor differences in the levels of both total and residual porewater pressures. Therefore it can be assumed

that the sand foundation is remarkably symmetrical in its properties about the centre line of the model.

Computed and Measured Acceleration Responses

The soil-structure interaction model was converted to prototype scale before analysis using TARA-3 and all data are quoted at prototype scale. Soil properties were consistent with relative density.

The computed and measured horizontal accelerations at the top of the structure at the location of ACC 1938 are shown in Fig. 38. They are very similar in frequency content, each corresponding to the frequency of the input motion given by ACC 3441 (Fig. 37). The peak accelerations agree fairly closely.

The vertical accelerations due to rocking as recorded by ACC 1900 and those computed by TARA-3 are shown in Fig. 39. Again, the computed accelerations closely match the recorded accelerations in both peak values and frequency content. Note that the frequency content of the vertical accelerations is much higher than that of either the horizontal acceleration at the same level in the structure or that of the input motion. This occurs because the foundation soils are much stiffer under the normal compressive stresses due to rocking than under the shear stresses induced by the horizontal accelerations.

Computed and Measured Porewater Pressures

The porewater pressures in the free field recorded by PPT 2851 are shown in Fig. 40. In this case the changes in the mean normal stresses are not large and the fluctuations of the total porewater pressure about the residual value are relatively small. The peak residual porewater pressure, in the

absence of drainage, is given directly by the pressure recorded after the earthquake excitation has ceased. In the present test, significant shaking ceased after 7 seconds. A fairly reliable estimate of the peak residual pressure is given by the record between 7 and 7.5 seconds. The recorded value is slightly less than the value computed by TARA-3 but the overall agreement between measured and computed pressures is quite good.

As the structure is approached, the recorded porewater pressures show the increasing influence of soil-structure interaction. The pressures recorded by PPT 2846 adjacent to the structure (Fig. 41) show somewhat larger oscillations than those recorded in the free field. This location is close enough to the structure to be affected by the cyclic normal stresses caused by rocking. The recorded peak value of the residual porewater pressure is given by the relatively flat portion of the record between 7 and 7.5 seconds. The computed and recorded values agree very closely.

Transducer PPT 2338 is located directly under the structure near the edge and was subjected to large cycles of normal stress due to rocking of the structure. These fluctuations in stress resulted in similar fluctuations in mean normal stress and hence in porewater pressure. This is clearly evident in the porewater pressure record shown in Fig. 42. The higher frequency peaks superimposed on the larger oscillations are due to dilations caused by shear strains. The peak residual porewater pressure which controls stability is observed between 7 and 7.5 seconds just after the strong shaking has ceased and before significant drainage has time to occur. The computed and measured residual porewater pressures agree very closely.

CONCLUSIONS

Reliable methods of analysis are available for estimating the seismic response of sites and some soil-structure systems. Reliable predictions of ground motions depend almost entirely on the degree to which the input motions for analysis can be estimated, especially in the absence of acceleration records from previous earthquakes at locations adjacent to the site.

The selection of representative motions for use as input in seismic response analyses requires considerable skill and a deep understanding of the role of system characteristics in defining seismic response. For important structures a sufficient number of candidate motions should be selected to ensure that a wide range in frequency content is explored. This increases the probability of including the frequency of possible future peak response. The final selection of design spectra is also helped by the knowledge of the sensitivity of the site response to various input frequencies in the neighbourhood of the critical structural periods. The practice of selecting just one or two candidate motions, which is unfortunately fairly common, may be dangerously unconservative.

The modelling of the incoming seismic waves as horizontal shear waves propagating vertically is inadequate wherever significant surface waves are likely. It may also be inadequately close to the epicentre.

Careful consideration should be given to how rock outcrop motions get into the soil layers. Substantial focussing and amplification may occur. The order of magnitude of these effects may be explored by 2-D dynamic analysis.

Nonlinear dynamic effective stress analysis provides a fundamental approach to the response analysis of soil structures and soil-structure interaction systems as it incorporates the more important factors controlling dynamic response. This approach allows the direct computation of seismically induced porewater pressures and takes their effects into account in computing permanent deformations, stresses and accelerations. The program TARA-3, which incorporates the effective stress method, has been validated extensively by means of data from seismic tests on centrifuged models. The response parameters computed by TARA-3 agree with those recorded in a variety of model tests within limits acceptable for engineering purposes.

ACKNOWLEDGEMENTS

The analyses of site response in Mexico City are part of a study being conducted for the Canadian Council on Earthquake Engineering. The development of TARA-3 was supported by the National Science and Engineering Research Council of Canada under Grant No. 1498 and by the Exxon Production and Research Company. The centrifuge tests were funded by the U.S. Nuclear Regulatory Commission through the European Office of the U.S. Army, London. Description of the centrifuge model test and related figures are used by permission of Cork Geotechnics Ltd. The text was typed by Mrs. Kelly Lamb.

REFERENCES

Biot, M.A. 1941. General Theory of Three-Dimensional Consolidation. J. Appl. Phys., 12, 155-64.

Dean, E.T.R. (1985). FLY-14 Program Suite - In Flight Data Handling and Analysis Manual, Internal Report, Cambridge University, Engineering Department.

Dikmen, S.U. and Ghaboussi, J. 1984. Effective Stress Analysis of Seismic Response and Liquefaction: Theory. Journal of the Geotech. Eng. Div., ASCE, Vol. 110, No. 5, Proc. Paper 18790, pp. 628-644.

Eyton, D.G.P. 1982. Triaxial Tests on Sand with Viscous Pore Fluid. Part 2, Project Report, Cambridge University, Engineering Department.

Finn, W.D. Liam, R. Siddharthan, F. Lee and A.N. Schofield. (1984). Seismic Response of Offshore Drilling Islands in a Centrifuge Including Soil-Structure Interaction. Proc., 16th Annual Offshore Technology Conf., Houston, Texas, OTC Paper 4693.

Finn, W.D. Liam. 1985. Dynamic Effective Stress Response of Soil Structures; Theory and Centrifugal Model Studies, Proc. 5th Int. Conf. on Num. Methods in Geomechanics, Nagoya, Japan, Vol. 1, 35-36.

Finn, W.D. Liam. 1986. Verification of Nonlinear Dynamic Analysis of Soils Using Centrifuged Models. Proc., International Symposium on Centrifuge Testing, Cambridge University, U.K., 20 pp.

Finn, W.D. Liam, R. Siddharthan, and R.H. Ledbetter. (1985a). Soil-Structure Interaction During Earthquakes, Proc. 11th Int. Conf. of the Int. Society of Soil Mech. and Found. Engineers, San Francisco, California, August 11-14.

Finn, W.D. Liam, R.S. Steedman, M. Yogendrakumar, and R.H. Ledbetter. (1985b). Seismic Response of Gravity Structures in a Centrifuge, Proc. 17th Annual Offshore Tech. Conf., Houston, Texas, OTC Paper 4885, 389-394.

Finn, W.D. Liam, Iai, S. and Ishihara, K. 1982. Performance of Artificial Offshore Islands Under Wave and Earthquake Loading: Field Data Analysis. Proceedings, Offshore Tech. Conf., Houston, Texas, OTC Paper No. 4220, Vol. I, pp. 661-672.

Finn, W.D. Liam, G.R. Martin and M.K.W. Lee. 1978. Comparison of Dynamic Analyses for Saturated Sands. Proceedings of the ASCE Specialty Conference on Earthquake Engineering and Soil Dynamics. Vol. I, ASCE, New York, N.Y., pp. 472-491.

Finn, W.D. Liam, M. Yogendrakumar, N. Yoshida, and H. Yoshida. 1986. TARA-3: A Program for Nonlinear Static and Dynamic Effective Stress Analysis, Soil Dynamics Group, University of British Columbia, Vancouver, B.C.

Goodman, R.E., R.L. Taylor and T.L. Brekke. 1968. A Model for the Mechanics of Jointed Rock, J. Soil Mech. and Found. Div. ASCE, 94 (SM3), 637-659.

Iai, S., Tsuchida, H. and Finn, W.D. Liam. 1985. An Effective Stress Analysis of Liquefaction at Ishinomaki Port During the 1978 Miyagi-Ken-Oki Earthquake. Report of the Port and Harbour Research Institute, Vol. 24, No. 2, June, pp. 1-84.

Ishihara, K., Shimizu, K. and Yasuda, Y. 1981. Porewater Pressures Measured in Sand Deposits During an Earthquake. Soils and Foundation Journal, Vol. 21, No. 4, December, pp. 85-100.

Lee, M.K.W. and Finn, W.D.L. 1975. DESRA-1, Dynamic Effective Stress Response Analysis of Soil Deposits. Dept. of Civil Engineering, University of British Columbia, Vancouver, B.C.

Lee, M.K.W. and Finn, W.D.L. 1978. DESRA-2, Dynamic Effective Stress Response Analysis of Soil Deposits with Energy Transmitting Boundary Including Assessment of Liquefaction Potential. Soil Mechanics Series No. 38, Department of Civil Engineering, University of British Columbia, Vancouver, B.C.

Leon, J.L., Jaime, A. and Tabago, A. 1974. Dynamic Properties of Soils - Preliminary Study. Institute of Engineering, UNAM, (in Spanish).

Lysmer, J., Udaka, T., Tsai, C.F. and Seed, H.B. 1975. FLUSH: A Computer Program for Approximate 3-D Analysis of Soil-Structure Interaction Problems. Report No. EERC 75-30, Earthquake Engineering Research Center, University of California, Berkeley, California.

Martin, G.R., W.D. Liam Finn, and H.B. Seed. 1975. Fundamentals of Liquefaction Under Cyclic Loading, Soil Mech. Series Report. No. 23, Dept. of Civil Engineering, University of British Columbia, Vancouver; also Proc. Paper 11284, J. Geotech. Eng. Div. ASCE, 101 (GT5): 324-438.

Martin, P.P. and Seed, H.B. 1978. MASH - A Computer Program for the Nonlinear Analysis of Vertically Propagating Shear Waves in Horizontaly Layered Soil Deposits. EERC Report No. UCB/EERC-78/23, Univ. of California, Berkeley, California, October.

Masing, G. 1926. Eigenspannungen und Verfestigung beim Messing, Proc., 2nd Int. Congress of Applied Mechanics, Zurich, Switzerland.

Ohta, T., Niva, M. and Andoh, H. 1977. Seismic Motions in the Deeper Portions of Bedrock and in the Surface and Response of Surface Layers. Proc., 4th Japan Earthquake Engineering Symposium, Tokyo, pp. 129-136 (in Japanese).

Prevost, J.H. 1981. DYNAFLOW: A Nonlinear Transient Finite Element Analysis Program. Princeton University, Department of Civil Engineering, Princeton, N.J.

Romo, M.P. and Seed, H.B. 1986. Analytical Modelling of Dynamic Soil Response in the Mexico City Earthquake of September 19, 1985. In The Mexico Earthquakes - 1985: Factors Involved and Lessons Learned. American Society of Civil Engineers, New York, N.Y., pp. 148-162.

Romo, M.P. and Seed, H.B. 1986. Analytical Modelling of Dynamic Soil Response in the Mexico City Earthquake of September 19, 1985. Presented at International Symposium on Mexican Earthquake, Mexico City. To be published in proceeding.

Schnabel, P.B., Lysmer, J. and Seed, H.B. 1972. SHAKE: A Computer Program for Earthquake Response Analysis of Horizontally Layered Sites. Report No. EERC 72-12, Earthquake Engineering Research Center, University of California, Berkeley, California.

Seed, H.B., Idriss, I.M. and Kiefer, F.W. 1969. Characteristics of Rock Motions During Earthquakes. Journal of Soil Mechanics and Foundations Division, ASCE, Vol. 95, No. 5, pp. 1199-1218.

Streeter, V.L., Wylie, E.B. and Richart, F.E. 1973. Soil Motion Computations by Characteristics Method. ASCE National Structural Engineering Meetings, San Francisco, California, Preprint 1952.

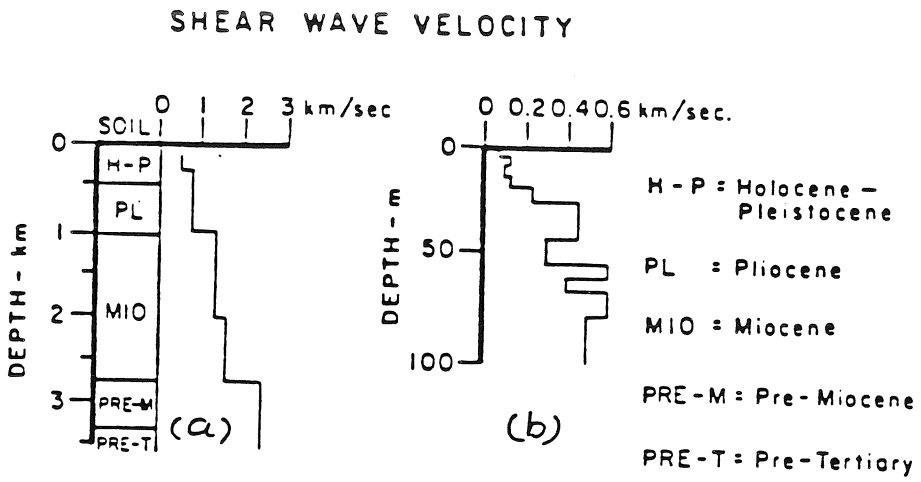

Figure 1. Geological profile of the test site.

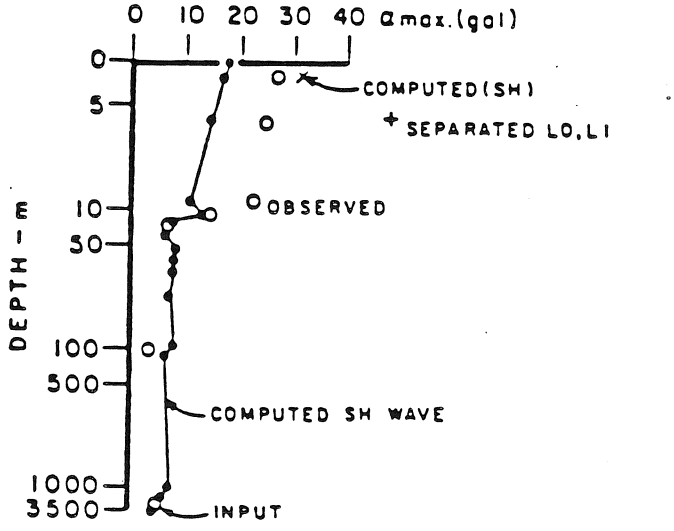

Comparison of computed and measured ground motions.

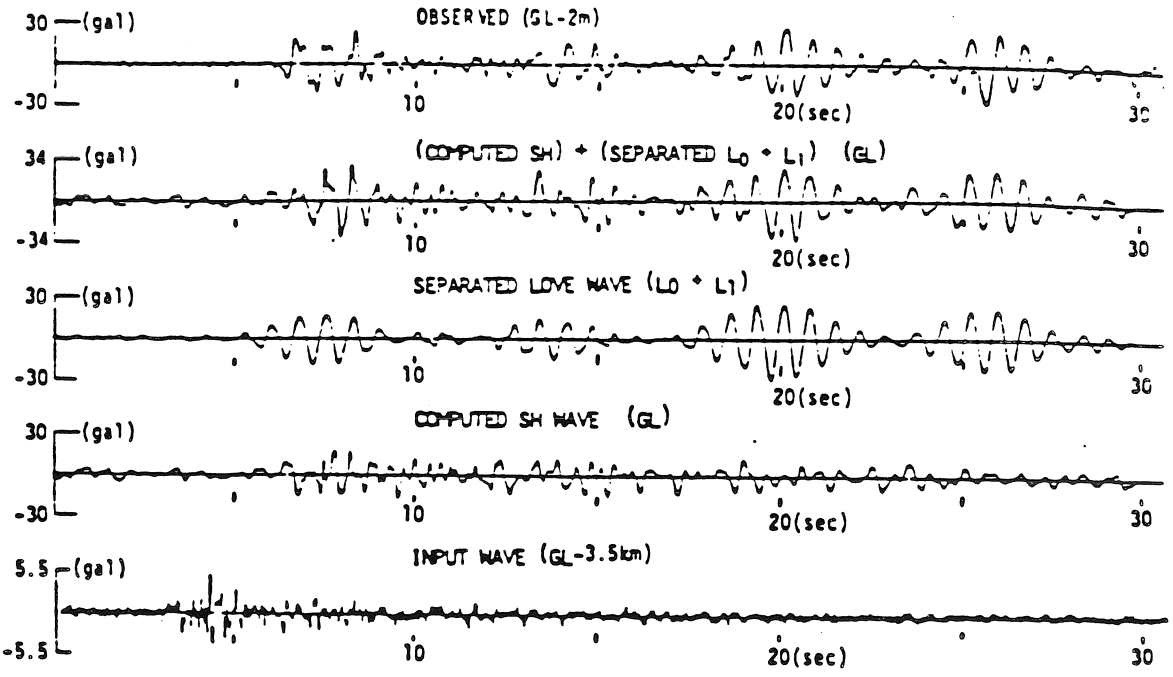

Figure 3. Computed and observed motions at the surface.

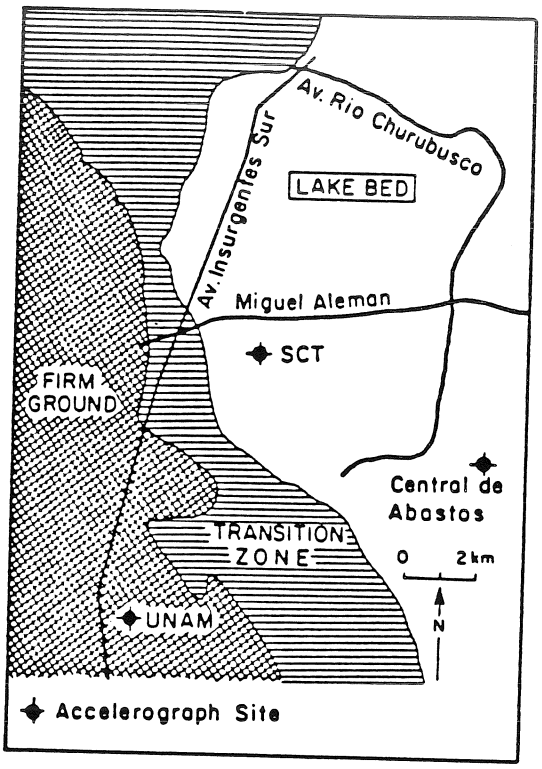

Figure 4. Soil zones and accelerograph sites in Mexico City (after Mitchell et al., 1986).

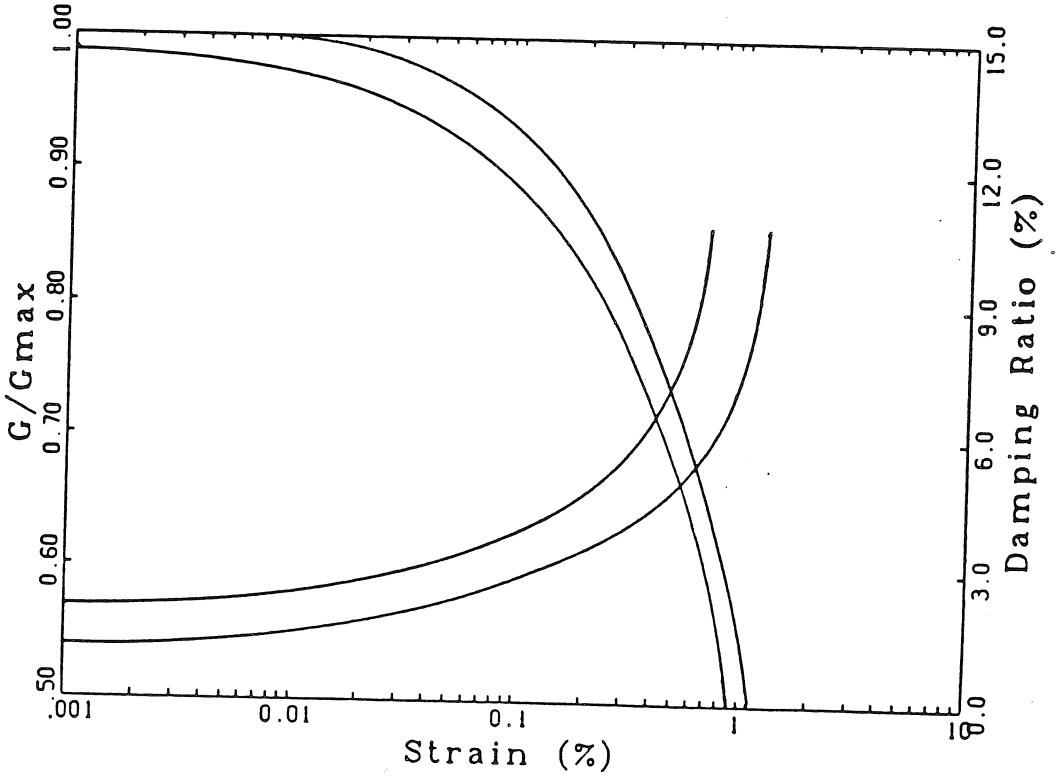

Figure 5. Range in shear-dependent moduli and damping for Mexico City clay (after Leon et al., 1974 and Romo and Jaime, 1986).

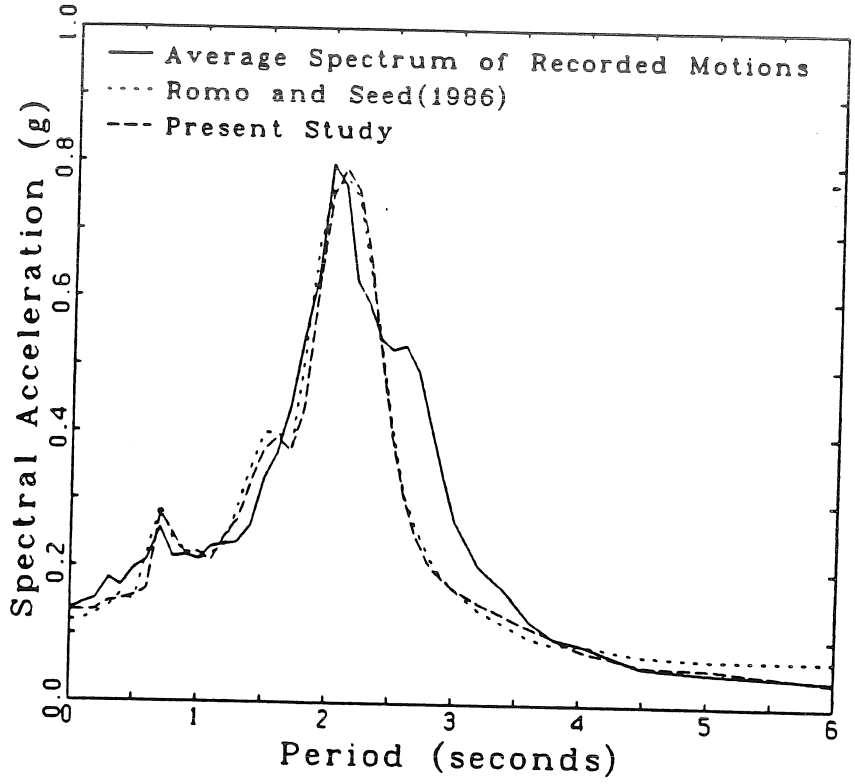

Figure 6. Response spectra (5% damping) of computed motions and average response spectra of the recorded motions at the SCT site.

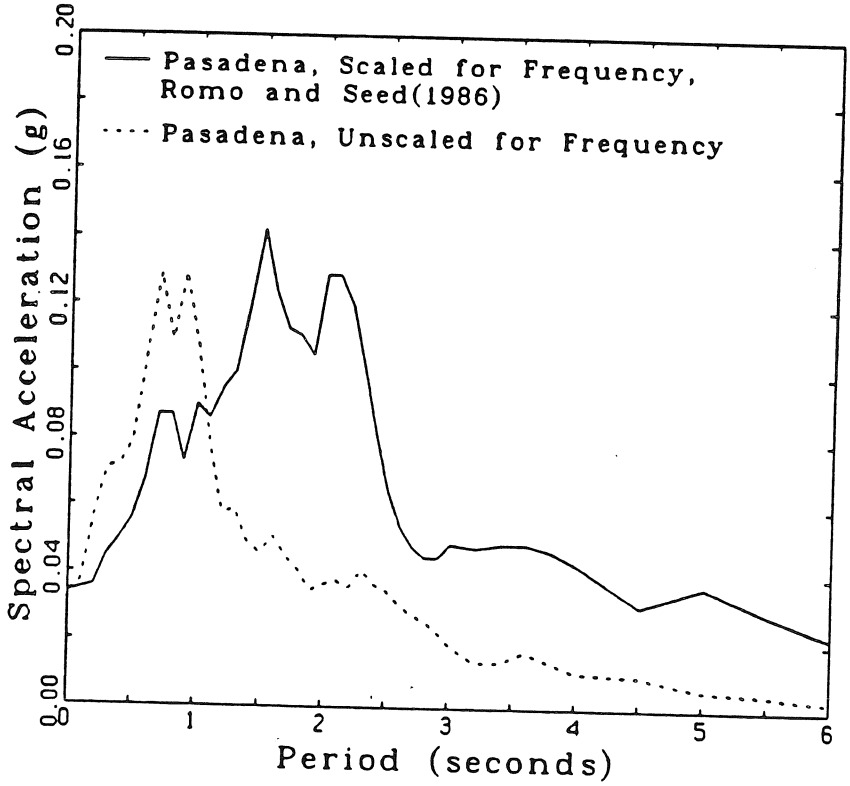

Figure 7. Response spectra (5% damping) for Pasadena record showing effect of frequency scaling.

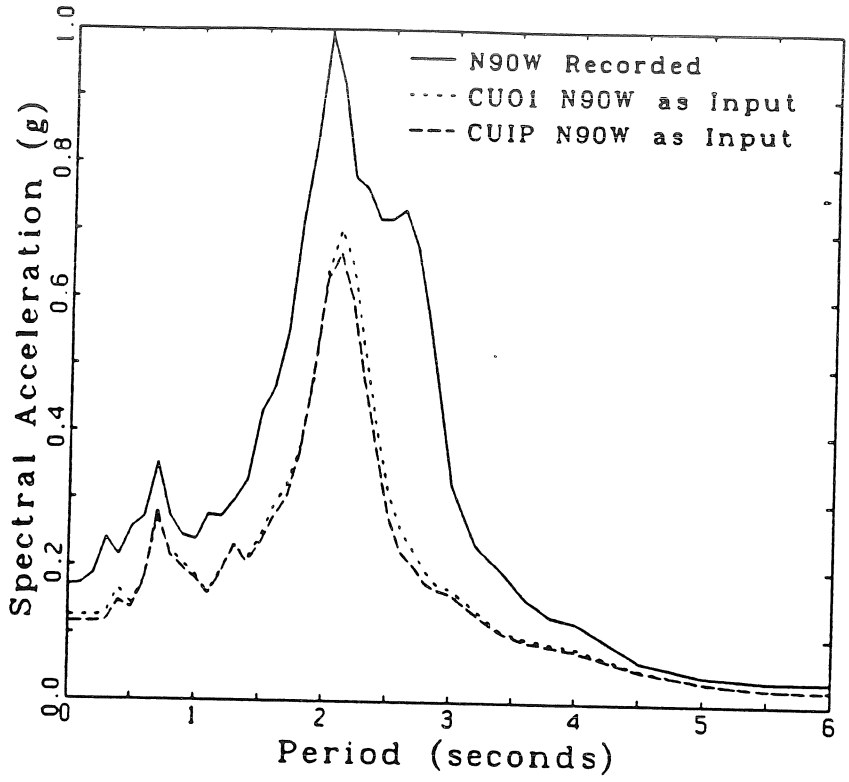

Figure 8. Response spectra (5% damping) of recorded and computed motions in the N90W direction at the SCT site.

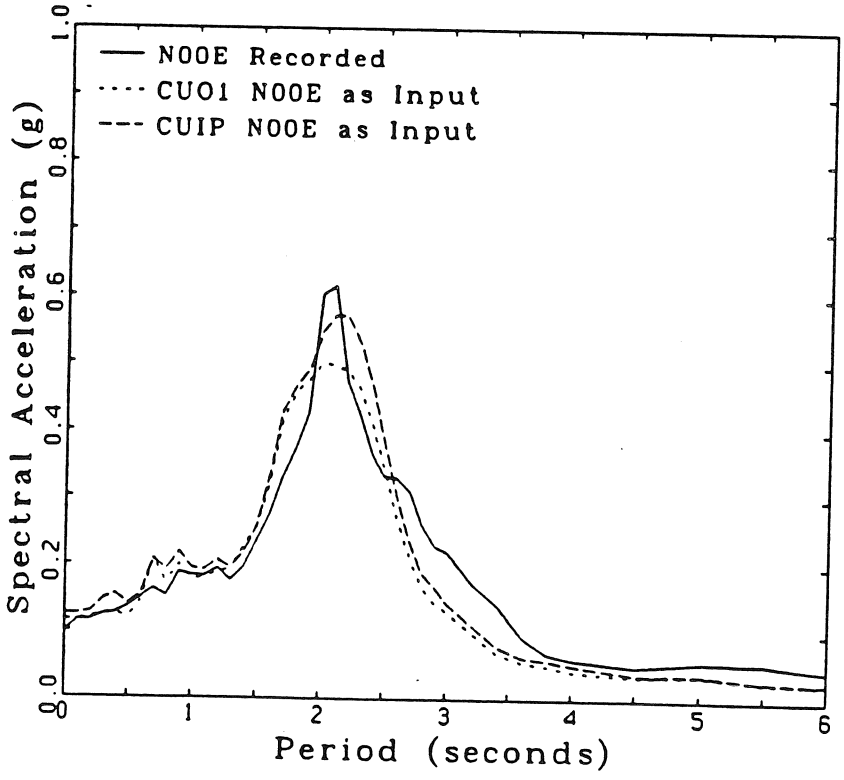

Figure 9. Response spectra (5% damping) of recorded and computed motions in the N00E direction at the SCT site.

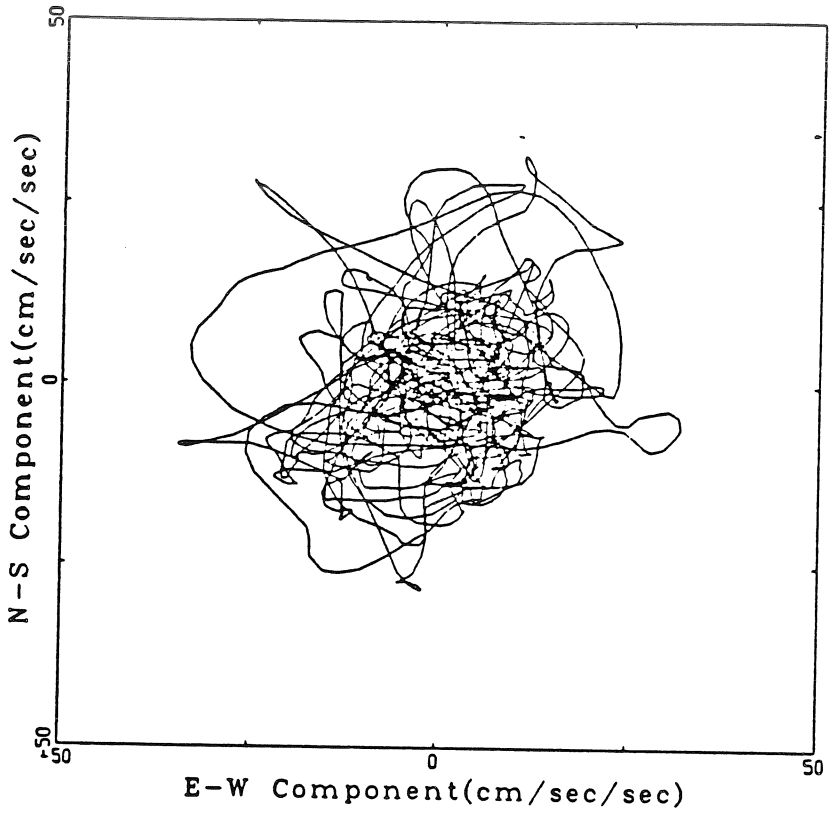

Figure 10a. Recorded accelerations at the CUIP site.

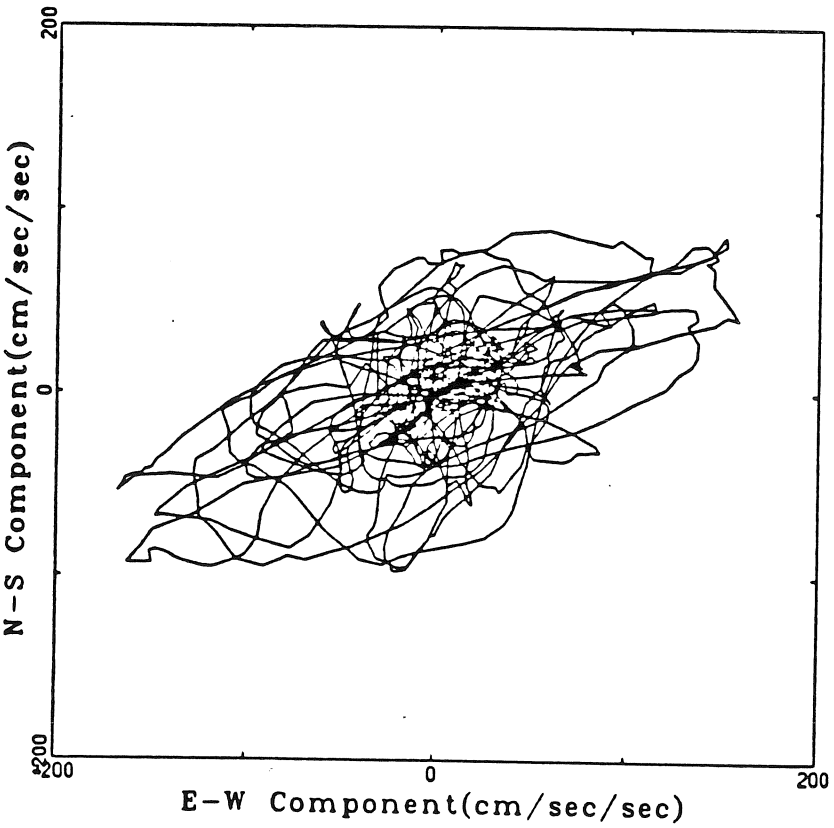

Figure 10b. Recorded accelerations at the SCT site.

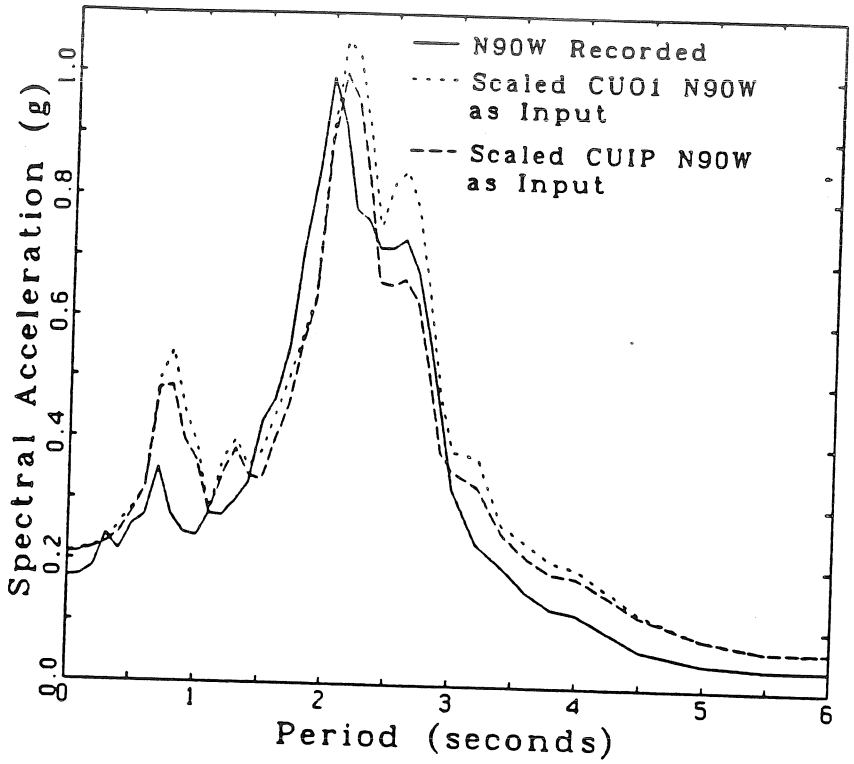

Figure 11. Response spectra (5% damping) of recorded and computed motions in the N90W direction at the SCT site, scaled outcrop motions as input.

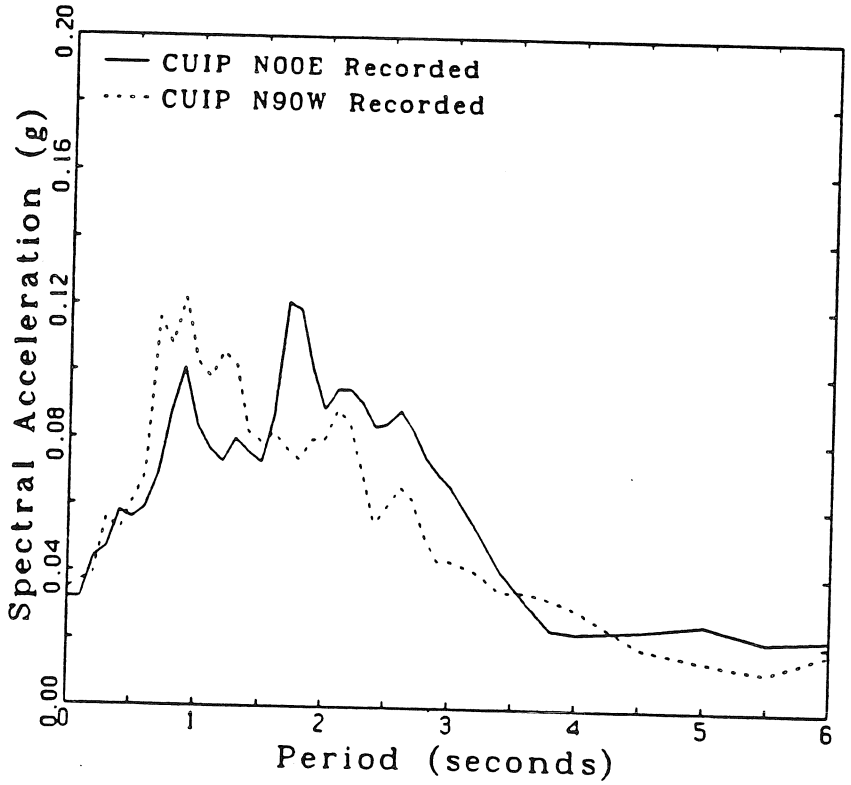

Figure 12. Response spectra (5% damping) of recorded motions at the CUIP site.

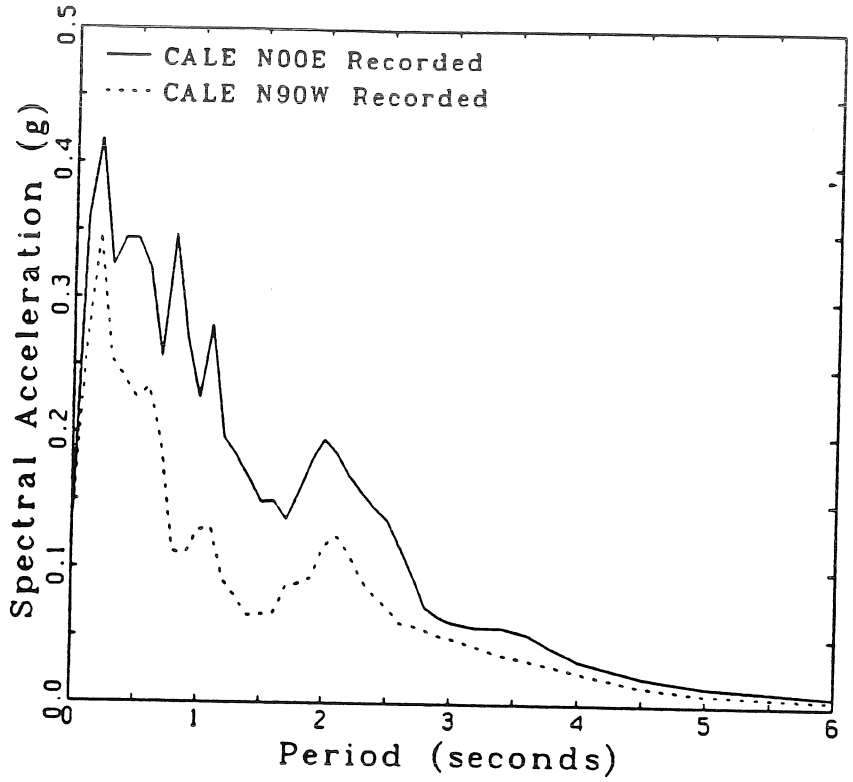

Figure 13. Response spectra (5% damping) of recorded motions at the Caleto de Campos site, 21 km from epicenter.

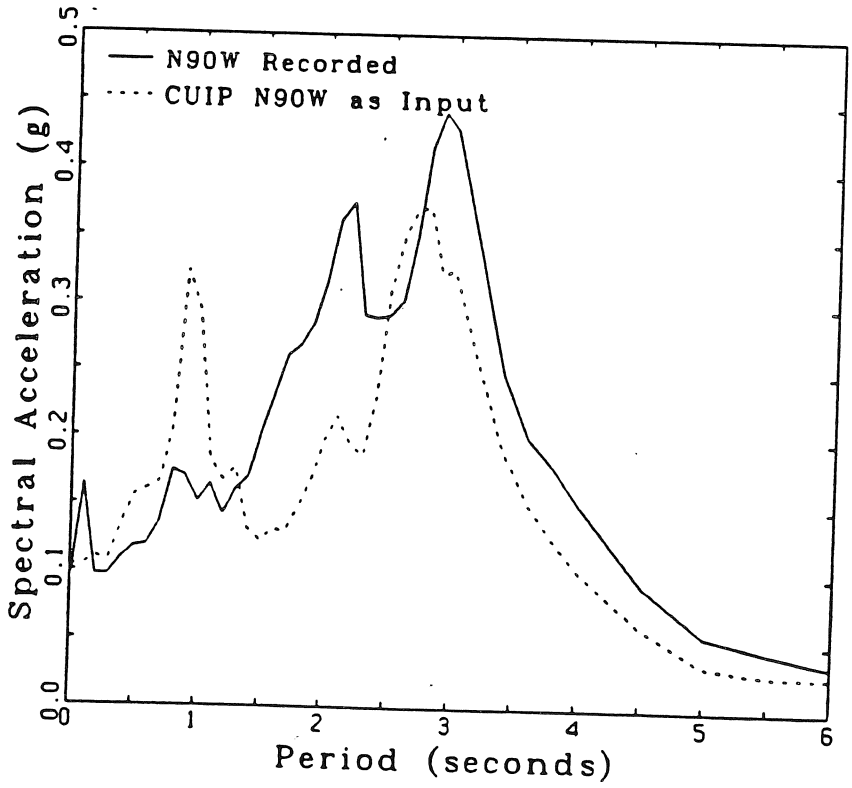

Figure 14. Response spectra (5% damping) of recorded and computed motions in the N90W direction at the CAF site.

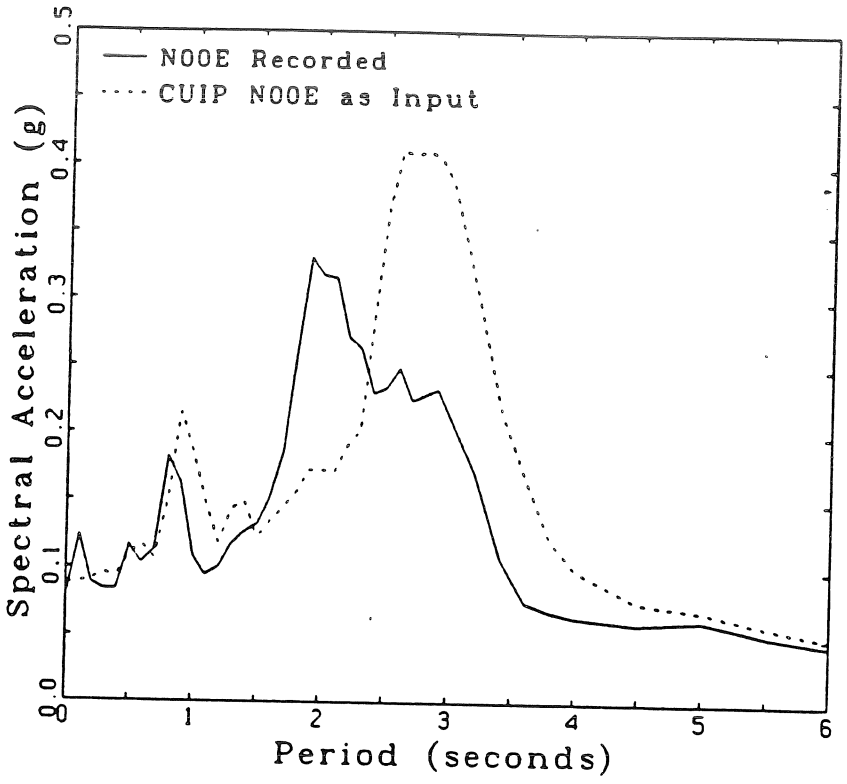

Figure 15. Response spectra (5% damping) of recorded and computed motions in the N00E direction at the CAF site.

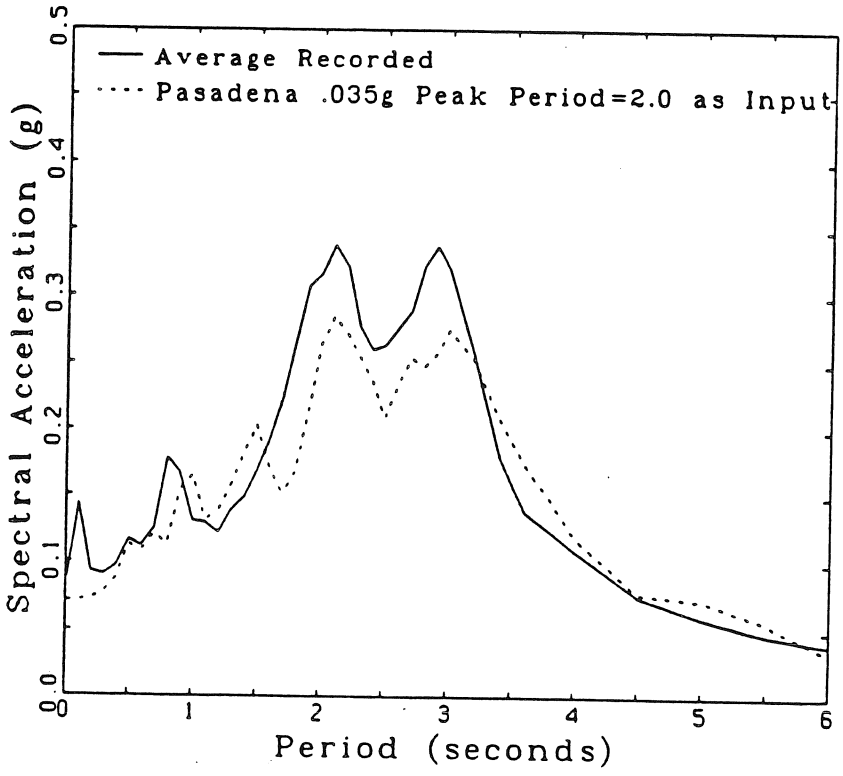

Figure 16. Response spectra (5% damping) of computed motions and average response spectra of the recorded motions at the CAF site.

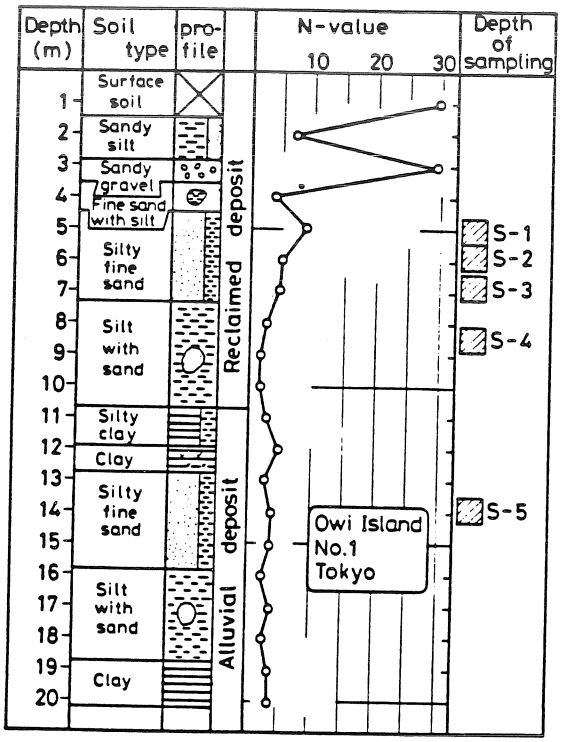

Figure 17. Soil profile at Owi Island.

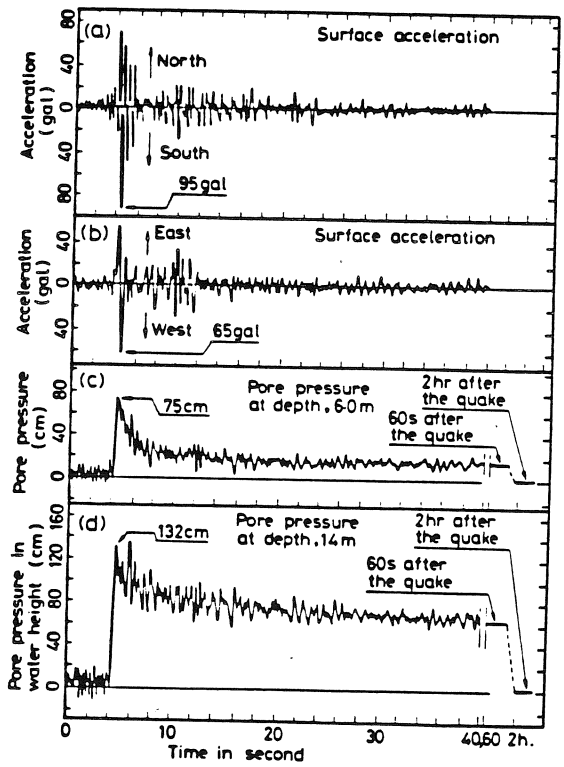

Figure 18. Recordings of accelerations and porewater pressure at Owi Island.

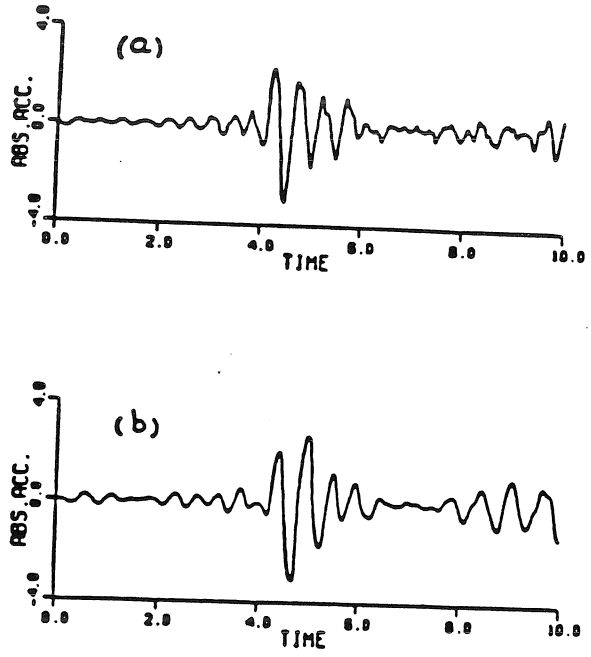

Figure 19. Recorded and computed accelerations at Owi Island.

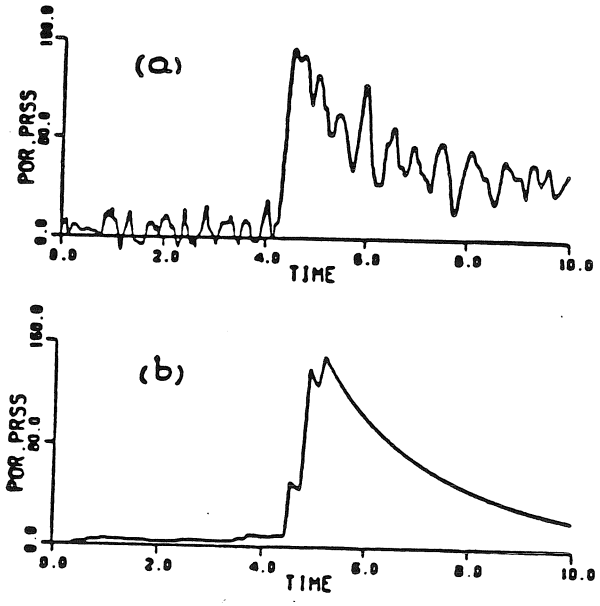

Figure 20. Recorded and computed porewater pressures at depth of 6 m.

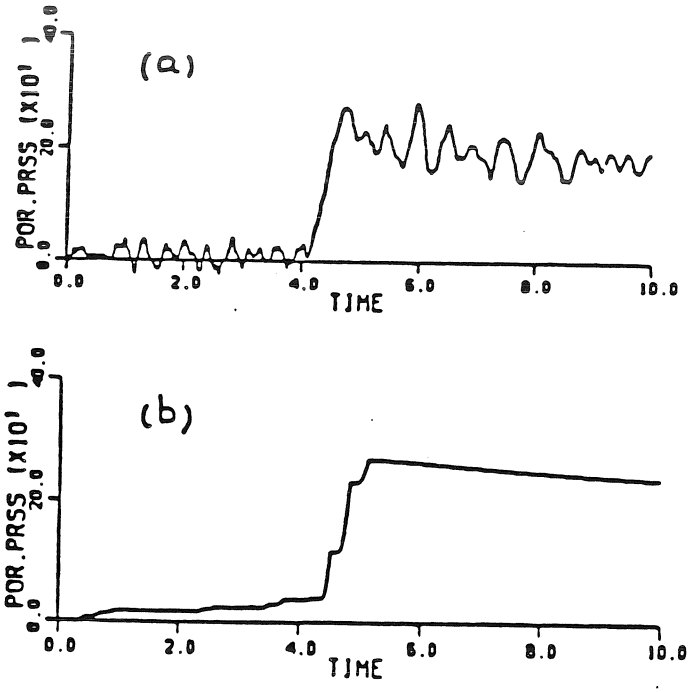

Figure 21. Recorded and computed porewater pressures at depth of 14 m.

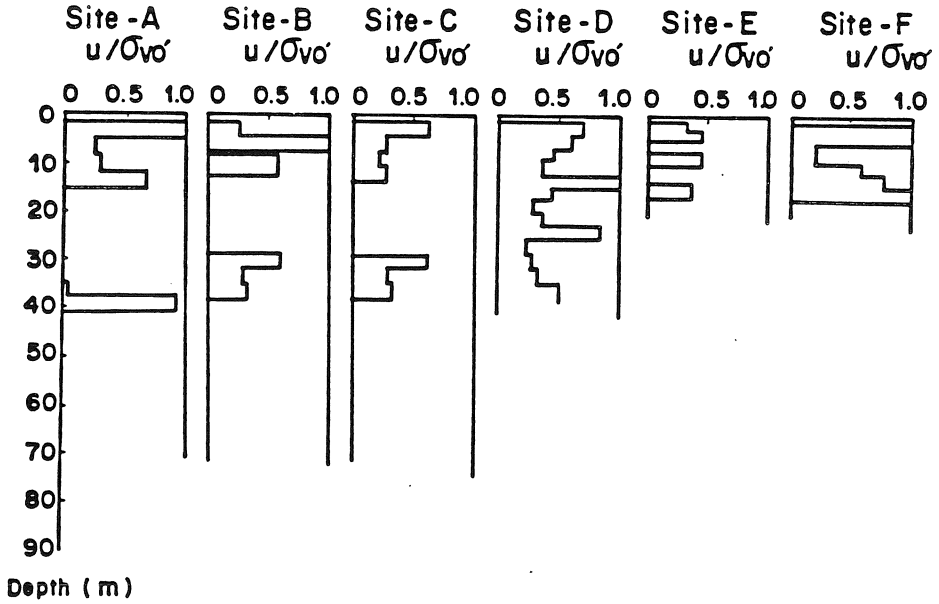

Figure 22. Computed porewater pressures at six Japanese sites.

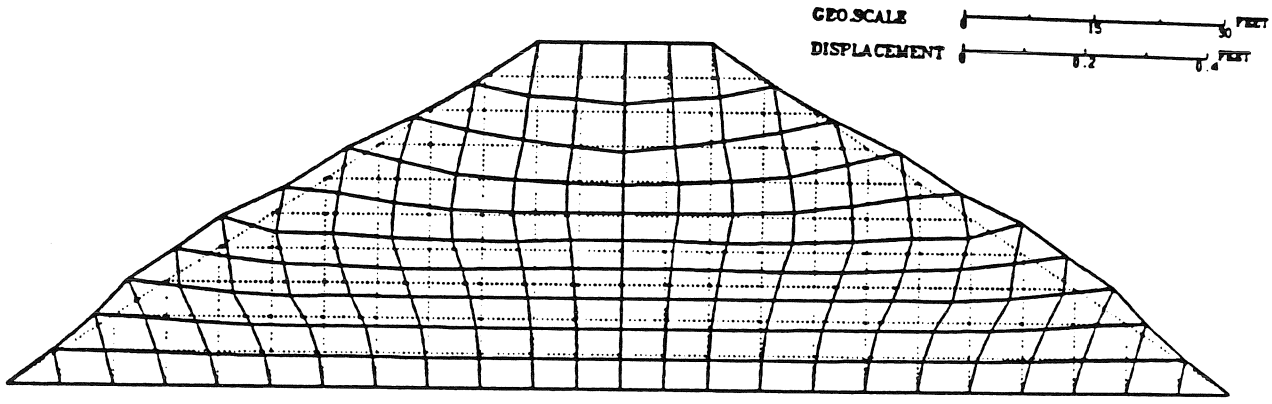

FIG. 23. Deformation of sand embankment during construction.

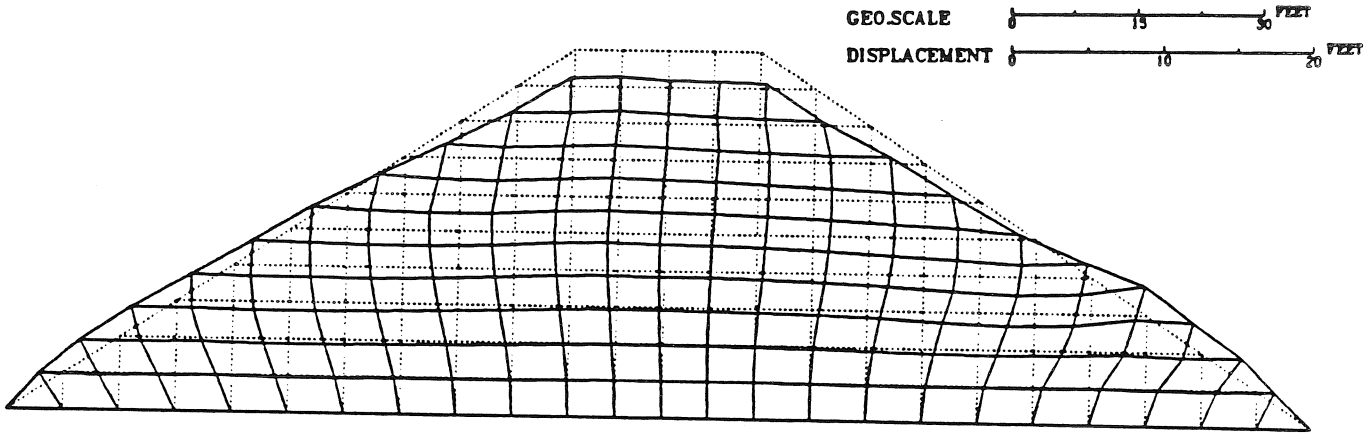

FIG. 24. Deformed shape of uniform embankment after earthquake.

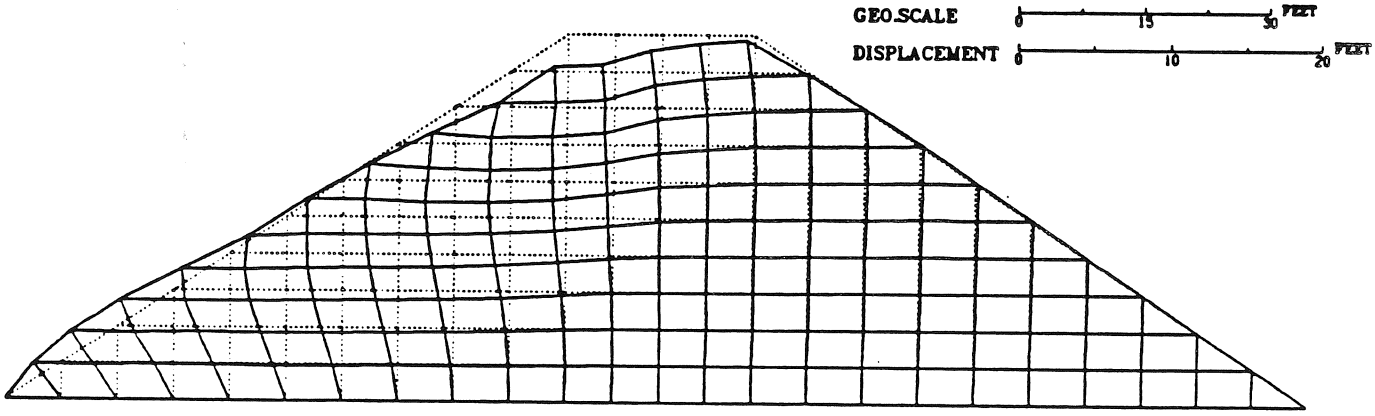

FIG. 25. Deformed shape of central core embankment after earthquake.

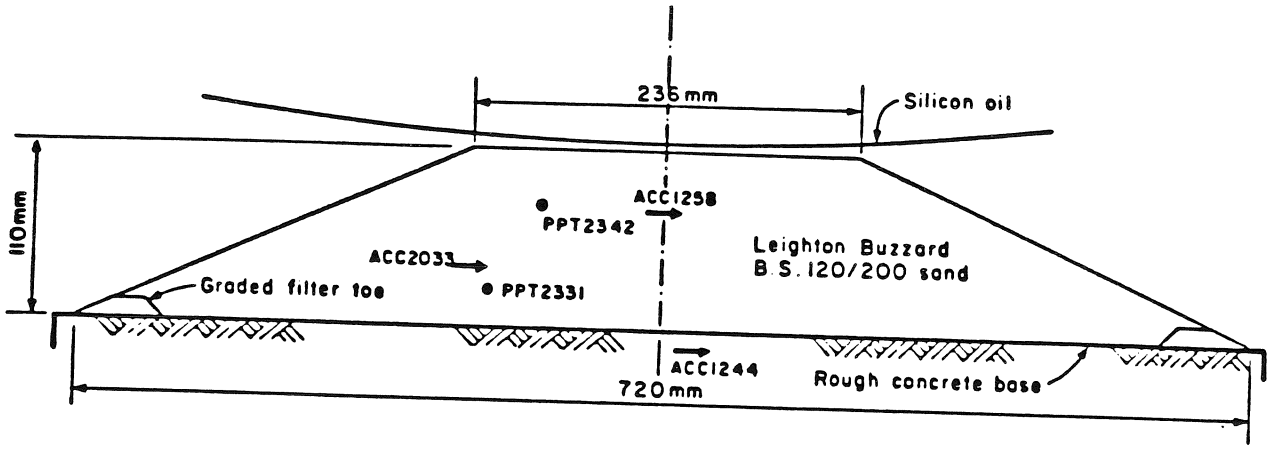

FIG. 26. Submerged model embankment showing instrumentation.

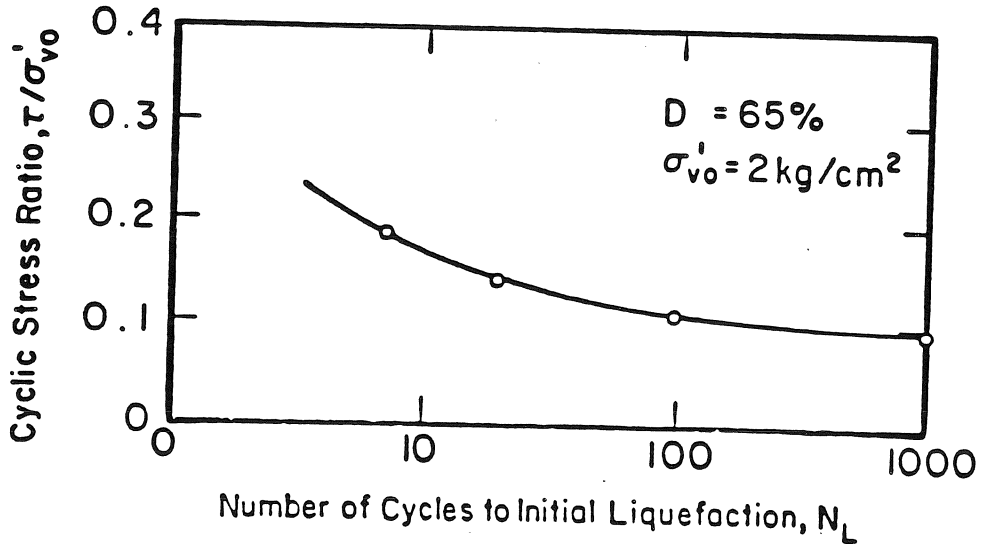

FIG. 27. Liquefaction curve for Leighton Buzzard sand at D_r = 65%.

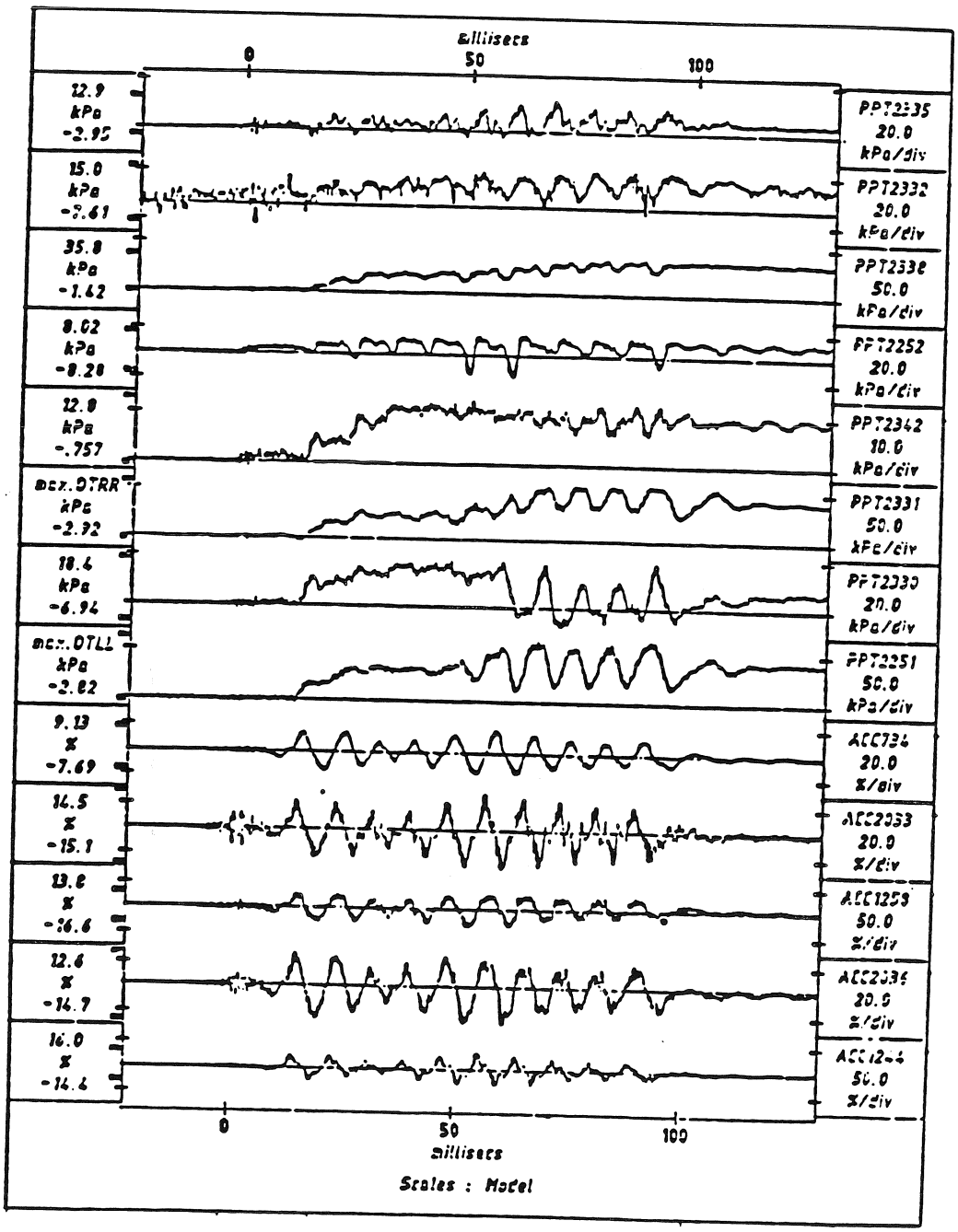

FIG. 28. Seismic data from saturated embankment.

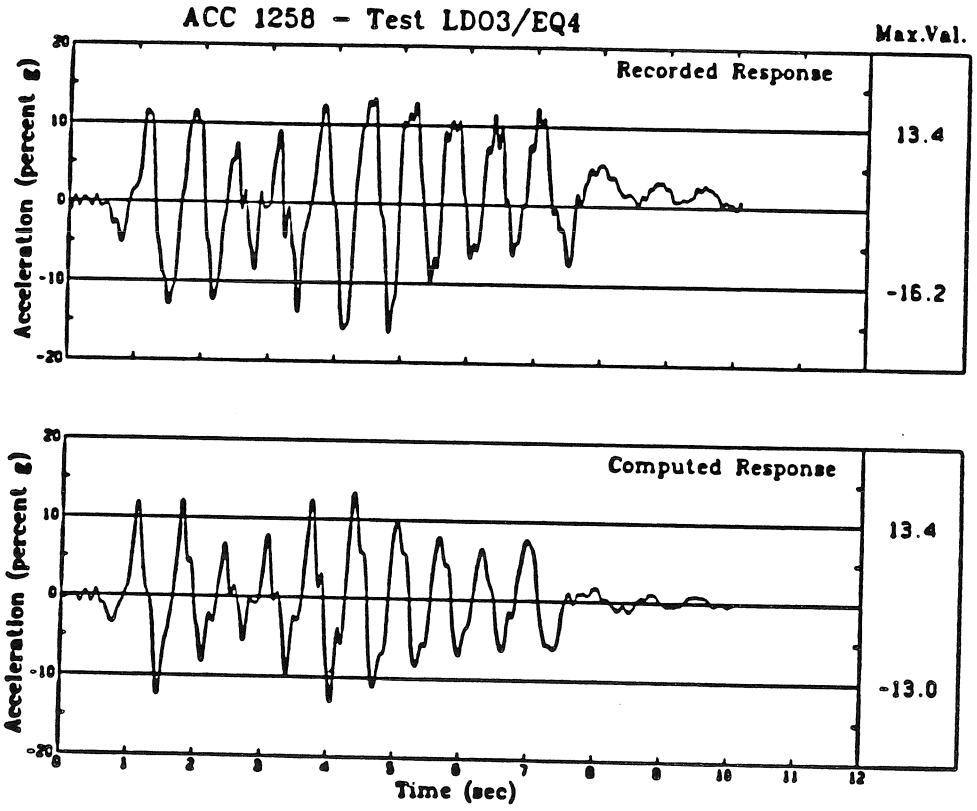

FIG.29. Measured and computed accelerations for ACC 1258.

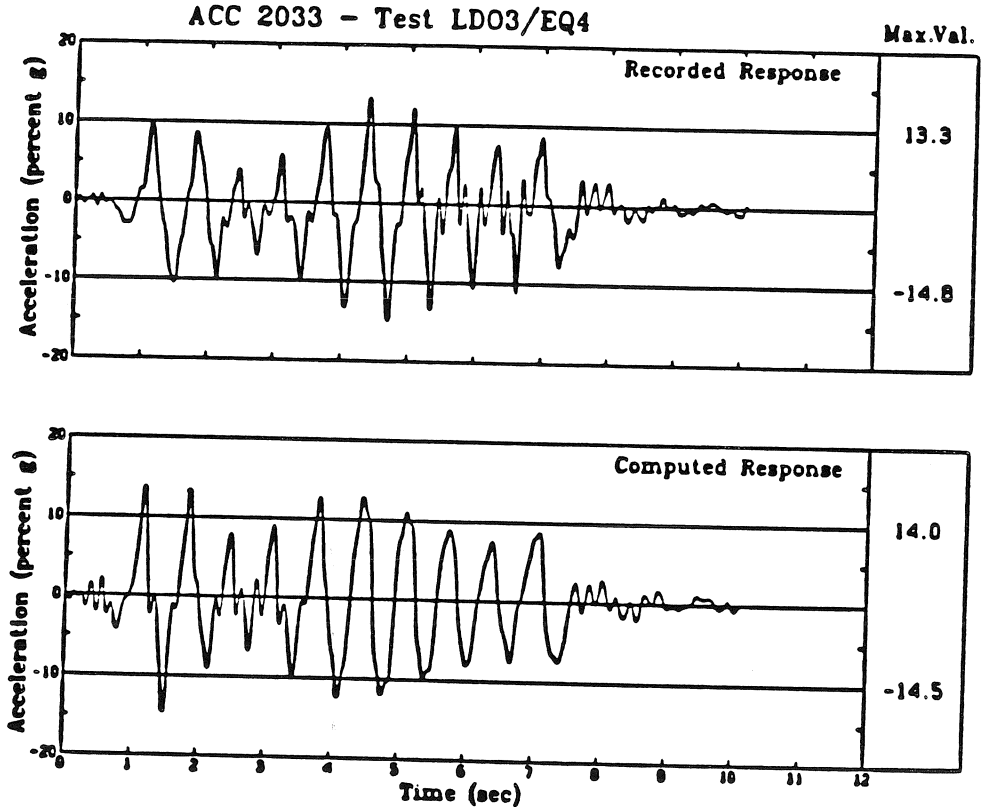

FIG. 30. Measured and computed accelerations for ACC 2033.

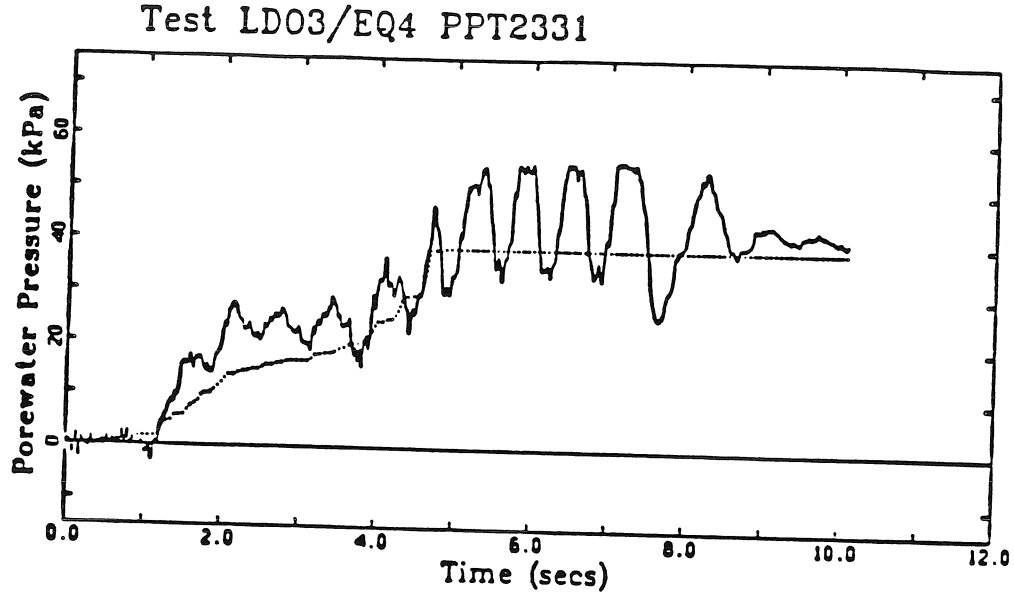

FIG. 31. Measured and computed porewater pressures at PPT 2331.

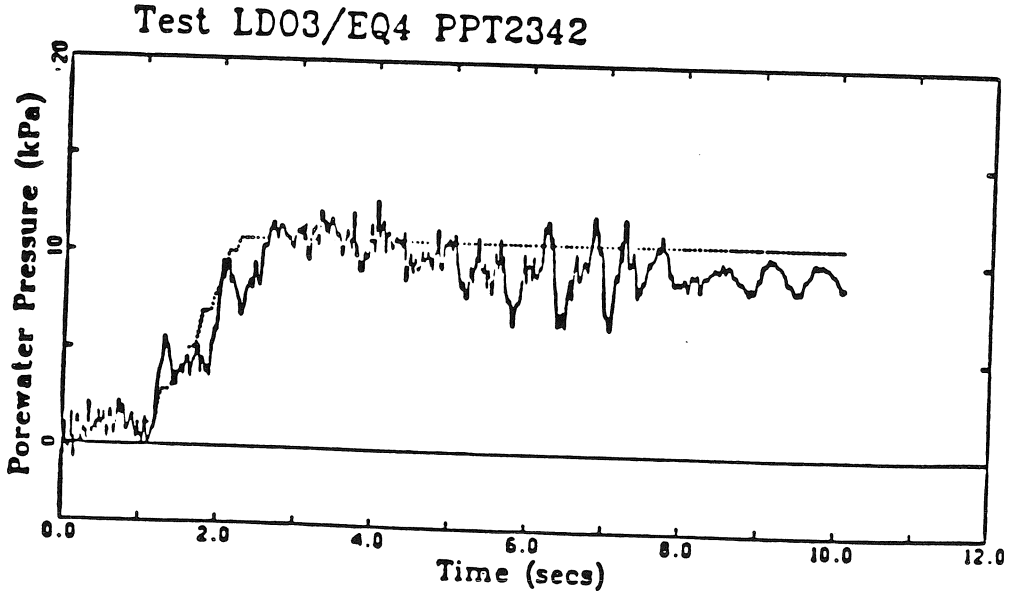

FIG. 32. Measured and computed porewater pressures at PPT 2342.

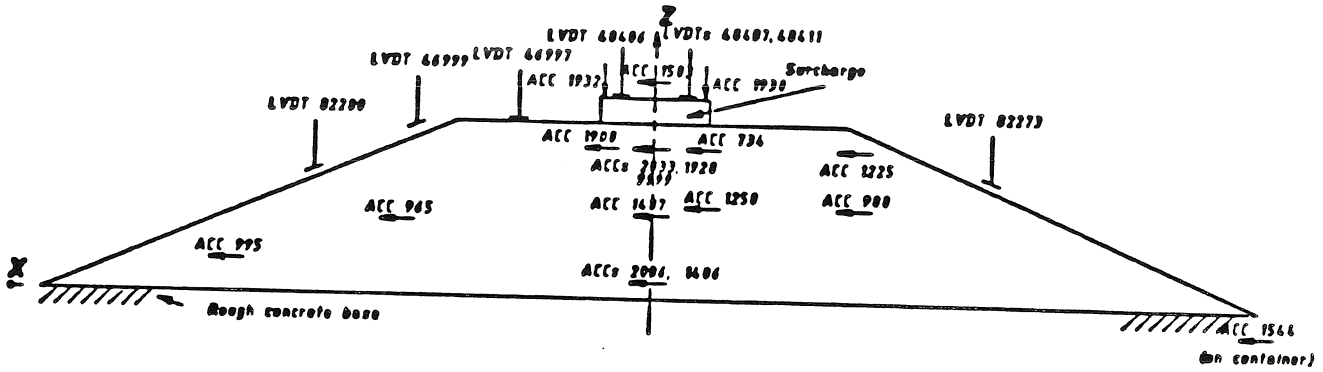

FIG. 33. Instrumented model of a surface structure in dry sand.

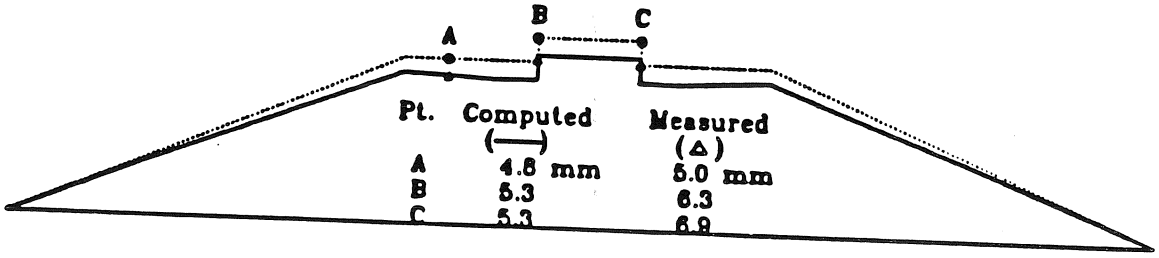

FIG. 34. Measured and computed settlements of surface structure in dry sand.

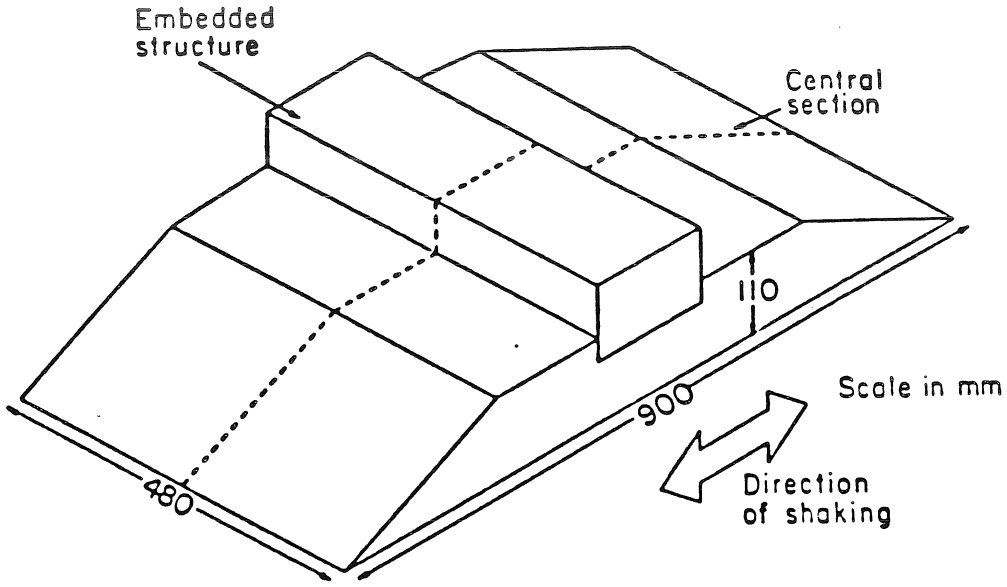

FIG. 35. Centrifugal model of embedded structure.

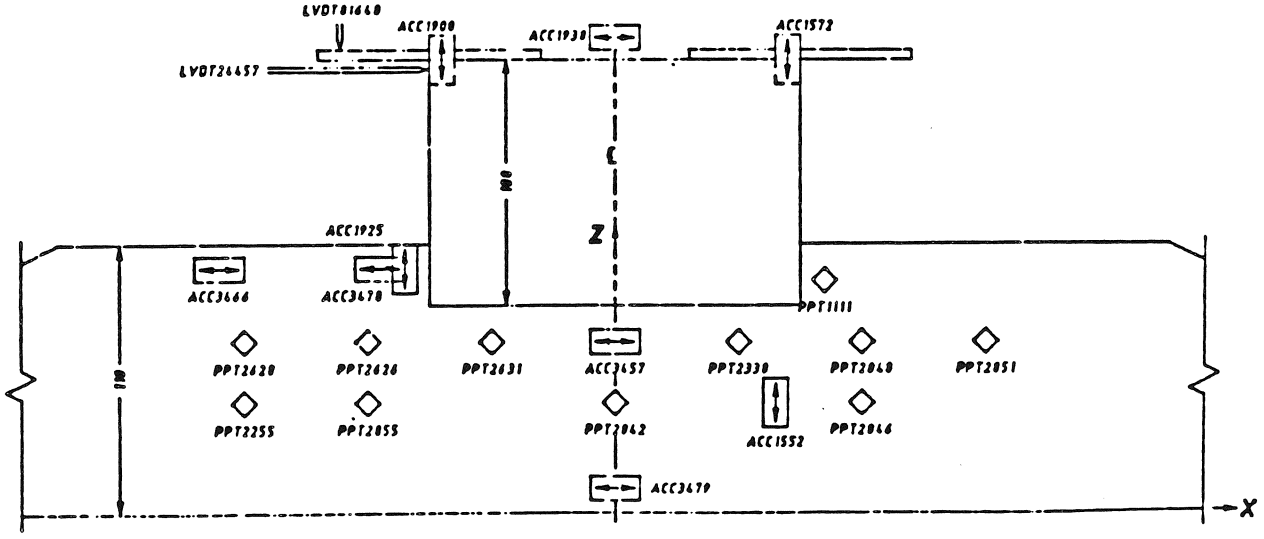

FIG. 36. Instrumented model of an embedded structure in saturated sand.

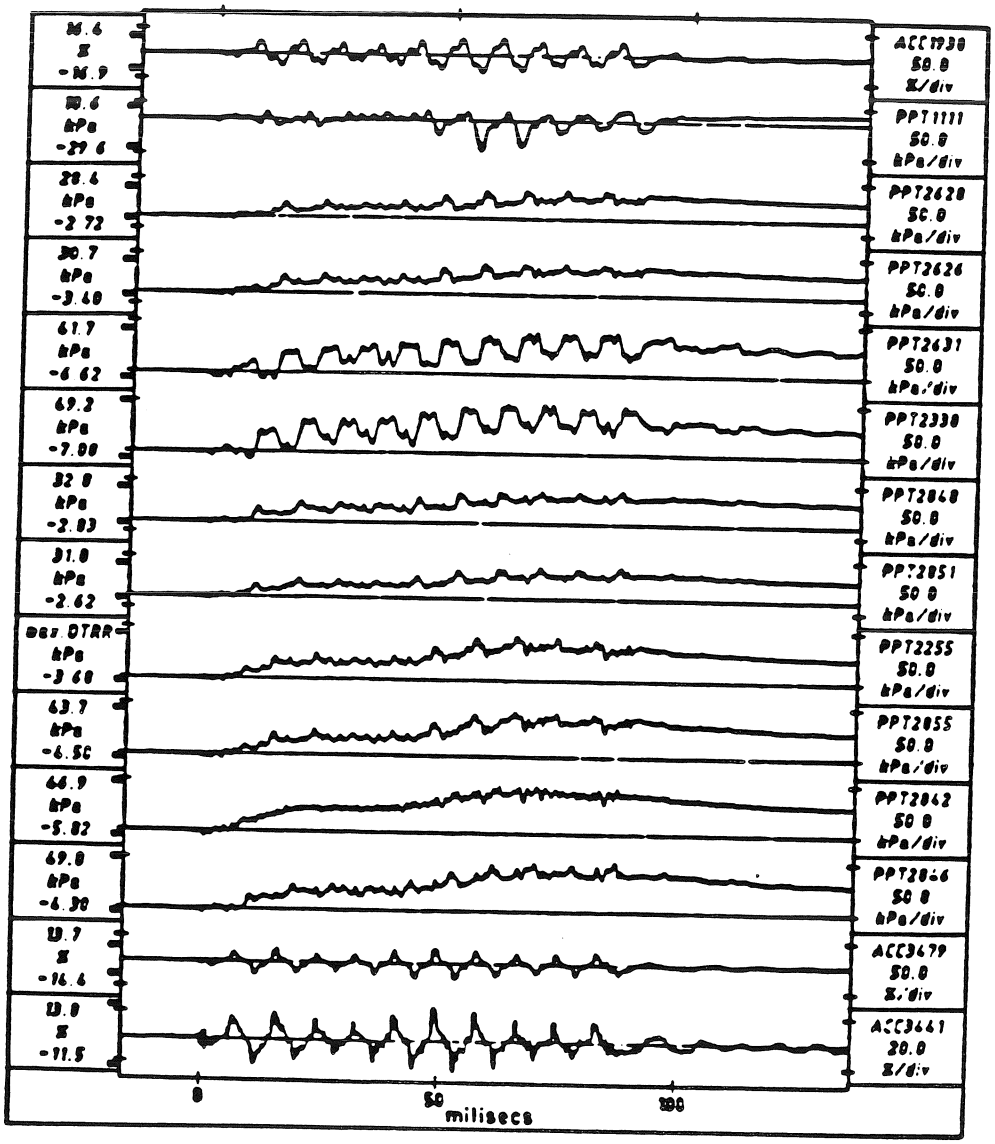

FIG. 37. Partial data from centrifuge test.

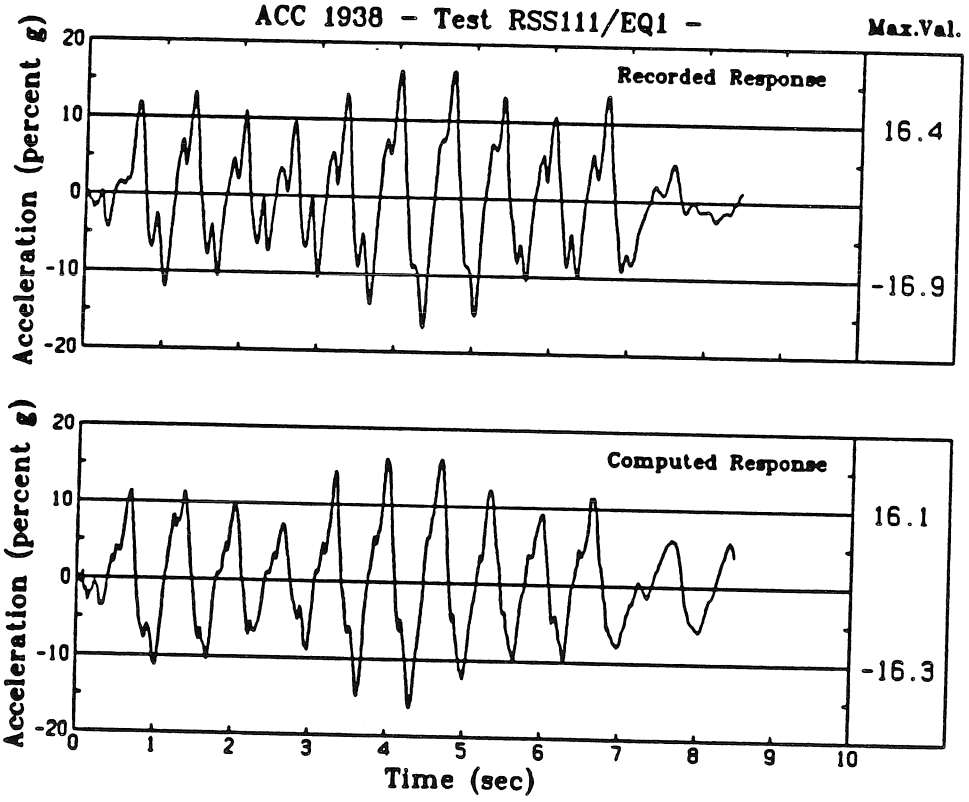

FIG. 38. Recorded and computed vertical accelerations at ACC 1938.

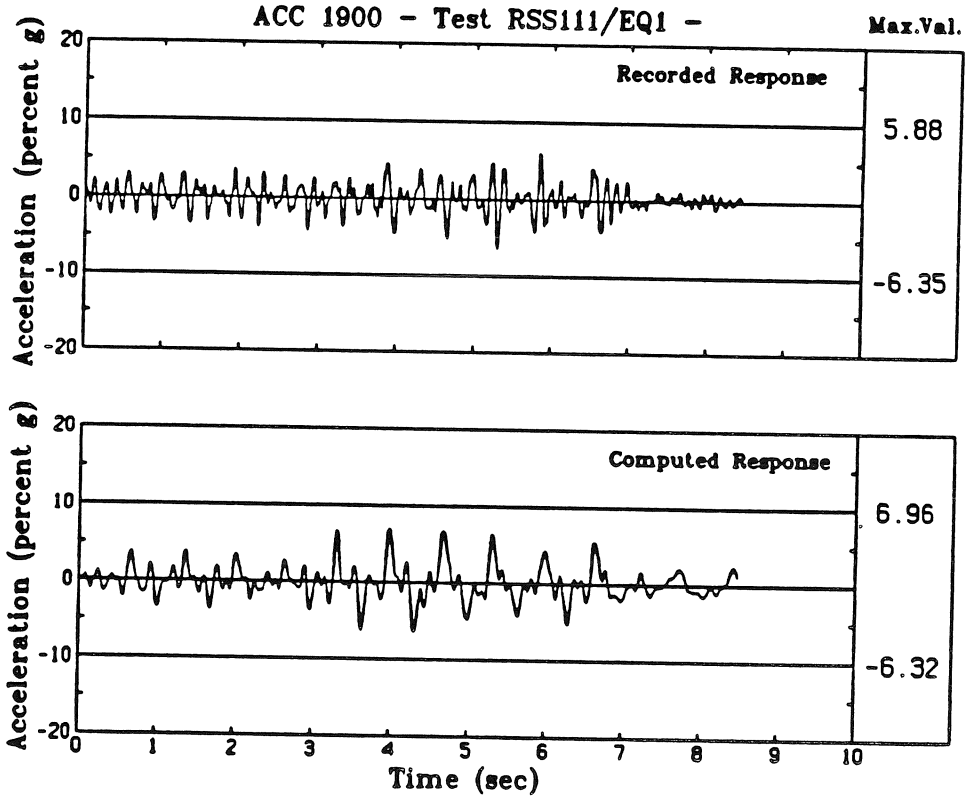

FIG. 39. Recorded and computed vertical accelerations at ACC 1900.

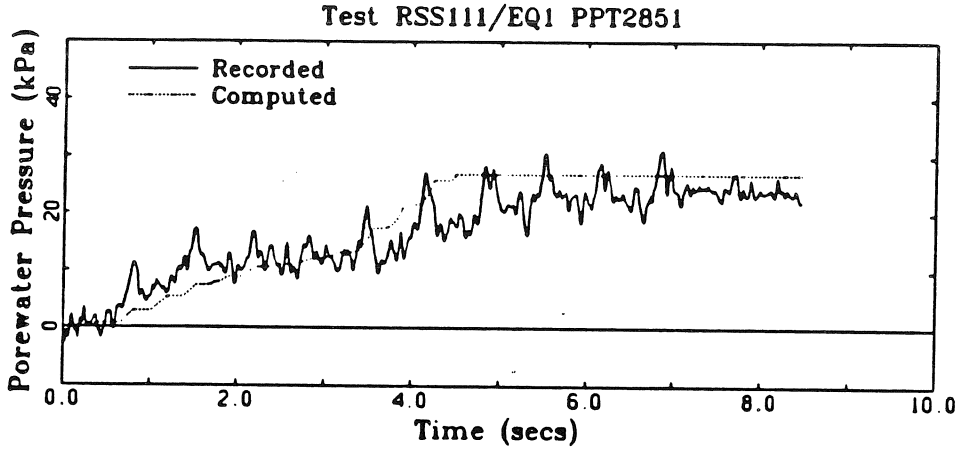

FIG. 40. Recorded and computed porewater pressures at PPT 2851.

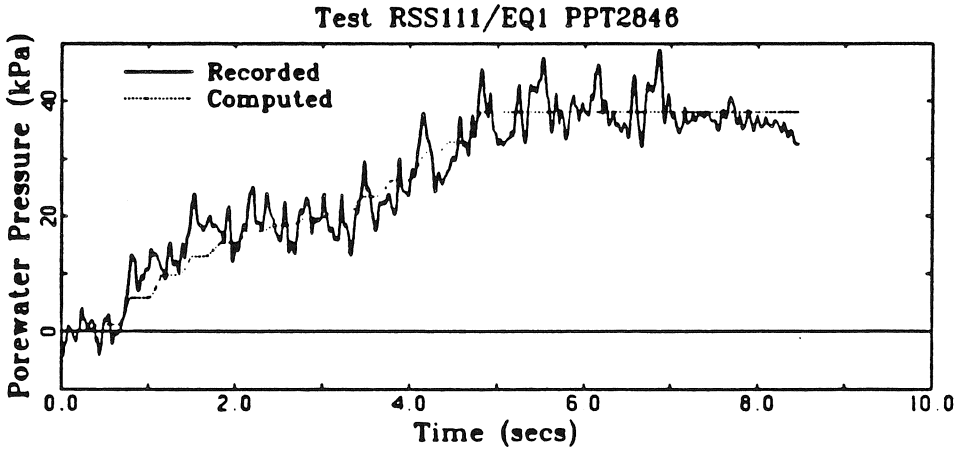

FIG. 41. Recorded and computed porewater pressures at PPT 2846.

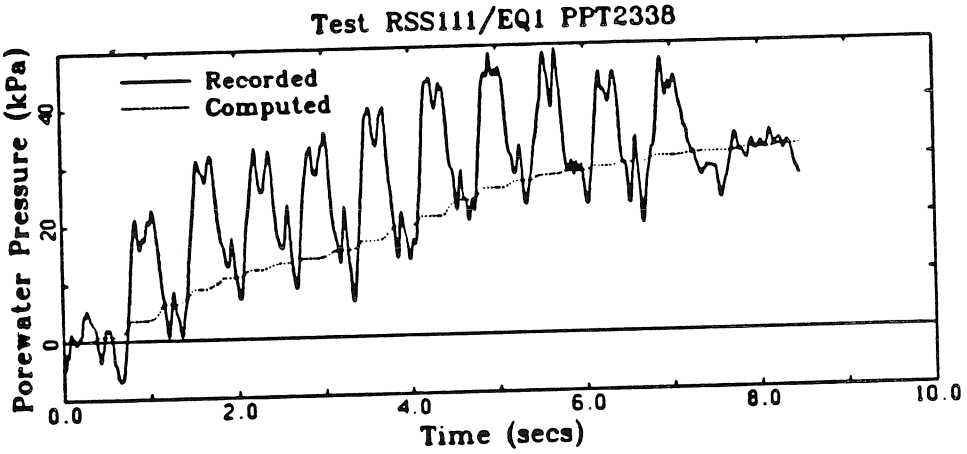

FIG. 42. Recorded and computed porewater pressures at PPT 2338.